Palaeogeography, Palaeoclimatology, Palaeoecology 457 (2016) 129–143

Contents lists available at ScienceDirect

Palaeogeography, Palaeoclimatology, Palaeoecology

journal homepage: www.elsevier.com/locate/palaeo

# The fate of diatom valves in the Subantarctic and Polar Frontal Zones of the Southern Ocean: Sediment trap versus surface sediment assemblages

Andrés S. Rigual-Hernández [a,*], Thomas W. Trull [b,c], Stephen G. Bray [b], Leanne K. Armand [a]

[a] Department of Biological Sciences, Macquarie University, North Ryde, NSW, 2109, Australia
[b] Antarctic Climate and Ecosystems Cooperative Research Centre, University of Tasmania, Hobart, Tasmania 7001, Australia
[c] CSIRO Oceans and Atmosphere Flagship, Hobart, Tasmania 7001, Australia

ARTICLE INFO

*Article history:*
Received 17 November 2015
Received in revised form 25 May 2016
Accepted 5 June 2016
Available online 7 June 2016

*Keywords:*
Diatoms
POC
Sediment traps
Surface sediments
Subantarctic Zone
Polar Frontal Zone

ABSTRACT

An array of deep ocean sediment traps was initiated in 1997 within the Australian sector of the Southern Ocean, and serviced annually for over a decade (the Subantarctic site is ongoing as part of the Southern Ocean Time Series). Here, we expand on previous findings obtained from the shallow traps (~1000 m depth) in the Polar Frontal Zone (PFZ) and Subantarctic Zone (SAZ) by examining the chemical composition and diatom assemblages collected by sediment traps deployed at bathypelagic depths in the PFZ (1500 m depth; years 1997–1998, 1999–2000 and 2003–2004) and SAZ (2000 and 3800 m; year 1999–2000). Additionally, the diatom assemblages of the surface sediments below the traps were analyzed to document how the seasonal signal is recorded in the sedimentary record. Analysis of the changes of the BSi:POC ratios with depth at both sites confirms previous work suggesting that the decoupling between Si and C cycles in the Southern Ocean is not different from other biogeochemical provinces of the world's ocean. Comparison of the seasonal flux pattern registered by the traps indicates that the diatom assemblages in the sediments of the Antarctic Zone and PFZ mainly represent the summer period. In contrast, the assemblages found in the sediments of the SAZ are a reflection of the spring and summer months, a period characterized by a larger variability in chemical and physical parameters. The strong correlation between the POC fluxes and the relative abundance of a group of diatom species (mainly *Pseudo-nitzschia* and small *Fragilariopsis*) in the PFZ traps suggest that there is an intimate relationship between the development of these species and the POC pulses to the deepest layers of the water column in this region. Interestingly, analysis of the diatom assemblages in the surface sediments reveals that the strong dissolution in the sediment-water interface removed the signal of these "carbon sinkers" from the sedimentary record leaving the sediment assemblage enriched in heavily silicified species.



## 1. Introduction

Diatoms represent one of the largest biomass producers on Earth, accounting for a significant fraction of the marine primary production (30–40%; Nelson et al., 1995; Tréguer et al., 1995; Buesseler et al., 2001). Diatoms use dissolved silica to build their skeletons (termed frustules) through biomineralization, making the greatest share of biogenic silica (BSi) produced in the world's ocean (Ragueneau et al., 2000; Tréguer and De La Rocha, 2013). Therefore, diatoms are an important component of the ocean's biological pump and silica cycle (Ragueneau et al., 2006) and may play an important role in regulating the exchange of $CO_2$ between the atmosphere and the ocean over various timescales (Sarmiento et al., 2004; Anderson et al., 2009).

The Southern Ocean represents the largest high-nutrient, low-chlorophyll (HNLC) region in the global ocean. The limited influence of surrounding land boundaries and generally low relief of the bottom topography in the Antarctic Circumpolar Current (ACC) result in extremely low iron concentrations in its surface waters, which restrict phytoplankton production (Jickells et al., 2005; Cassar et al., 2007; Tagliabue et al., 2014). Despite the overall low algal biomass accumulation, moderate increases in diatom abundances are often reported during spring and summer across the iron-limited waters of the ACC (e.g. Fischer et al., 2002; Green and Sambrotto, 2006; Grigorov et al., 2014). This diatom growth takes up the bulk of the silicic acid upwelled in the ACC eventually forming extensive diatom oozes on the sea floor. Indeed, the burial of diatom BSi in the Southern Ocean constitutes the single most important sink for silica in the world's ocean, accounting for about one third of the total global marine BSi accumulation (Tréguer and De La Rocha, 2013; Tréguer, 2014). The diatom remains preserved in these deep-sea sediments carry imprints of the habitats in which they were produced (e.g. Sea Surface Temperature - SST, sea-ice cover and iron availability). Therefore, diatom frustules are widely used in palaeoceanographic and palaeoclimatic reconstructions (e.g. Gersonde

* Corresponding author.
*E-mail address:* andres.rigualhernandez@gmail.com (A.S. Rigual-Hernández).

http://dx.doi.org/10.1016/j.palaeo.2016.06.004
0031-0182/

and Zielinski, 2000; Gersonde et al., 2005; Crosta et al., 2008; Armand and Leventer, 2010; Ferry et al., 2015), particularly in high latitude systems where calcareous micro- and nano-fossils are often missing or not systematically identified (Perch-Nielsen, 1985).

However, several physical, chemical and biological processes can severely alter the original diatom assemblage complicating the interpretation of the sedimentary record. Some of these processes include lateral transport by currents, dissolution, selective grazing and sediment winnowing and refocusing (e.g. Sancetta, 1989; Boltovskoy et al., 1993; Nees et al., 1999; Grigorov et al., 2014). Among these processes, dissolution of the frustule in the water column and at the sediment-water interface is probably the main factor responsible for the differences between the living diatom assemblages and those preserved in the sedimentary record (Ragueneau et al., 2000; Jordan and Stickley, 2010). After cell death, the organic coating that protects the living diatom cell is degraded by microbial activity, leaving the frustule exposed to dissolution in the water column (Passow et al., 2003). The dissolution of the amorphous silica of the naked diatom frustules depends on the degree of saturation of silicate (Hurd, 1972; Hurd and Birdwhistell, 1983), temperature (Kamatani, 1982) and surface area of silica exposed to seawater (Hurd and Birdwhistell, 1983). The dissolution rate is also influenced by the formation of aggregates and selective grazing, which can increase or diminish the rate of silica dissolution in surface waters depending on the grazer (Dugdale et al., 1995; Nelson et al., 1995; Brzezinski et al., 1997; Dugdale and Wilkerson, 1998). Whereas some zooplankton feeders such as large copepods and euphausiids, crunch the diatom cells producing small fragments that enhance dissolution processes (Hamm et al., 2003), others can ingest entire diatom frustules and produce faecal pellets that can act to protect the diatom cells from dissolution (Gauld, 1957; Yoon et al., 2001).

The aforementioned processes also influence the strength of the biological pump. In the Southern Ocean, the fraction of $CO_2$ dissolved in the mixed layer would re-equilibrate with the atmosphere within months, but the portion sinking to deeper layers and sediments will remain at depth for centuries or longer (Trull et al., 2001a; Smetacek et al., 2012). Thus, the depth at which the cell content of diatoms is remineralized determines the timescales during which the photosynthetically fixed $CO_2$ is sequestered from the atmosphere (Smetacek et al., 2012). Some robust and dissolution-resistant diatom taxa, such as the resting spores of *Chaetoceros* (*Chaetoceros* RS), *Thalassiosira* and *Eucampia antarctica*, have been reported to be able to bypass the mixed layer intact, therefore exporting their cell content to the ocean interior (Salter et al., 2012; Rynearson et al., 2013; Rembauville et al., 2014) where carbon can remain for long periods of time. Conversely, the frustule and cell contents of lightly silicified diatoms are normally readily recycled in the surface layer (unless aggregated and/or ballasted by heavier particles) allowing the remineralized carbon to re-equilibrate with the atmosphere on shorter timescales.

For these reasons, understanding the processes that diatom assemblages undergo from their initial production in the surface layer until their eventual preservation in the sediments is of critical importance to assess the information preserved in the sedimentary record and to determine the role of diatoms in the biological pump and cycling of silica. Analysis of the diatom assemblages captured by the sediment traps at different depths and in the surface sediments can be used to monitor the changes that diatom assemblages and the labile components of the flux undergo from their initial production in the upper water column until their preservation in the sediments (e.g. Abelmann and Gersonde, 1991; Honjo et al., 2000; Fischer et al., 2002; Romero and Armand, 2010; Grigorov et al., 2014). This coupled approach can help us to understand the processes occurring in the water column and the functioning of the biological pump. Moreover, this understanding is also needed to assess the usefulness of diatoms as indicators of palaeoclimatic and palaeoceanographic reconstructions.

In this study we report on diatom and biogenic particle fluxes collected by vertically moored sediment traps deployed in the Polar Frontal Zone (PFZ) and the Subantarctic Zone (SAZ) south of Tasmania. We expand on Rigual-Hernández et al. (2015b) findings in the upper ~1000 m of the water column by adding new information on the diatom and biogenic particle fluxes registered by the deeper traps in the PFZ (1500 m) and SAZ (2000 and 3800 m). Additionally, we compare the diatom assemblages registered by the traps with those found in the underlying sediments in order to determine how the seasonal signal on diatom production is recorded in the sedimentary record. Our results will allow for better interpretation of the fossil record in the SAZ and PFZ of the Southern Ocean.

## 2. Regional setting and methods

### 2.1. Oceanographic and biological setting

The Southern Ocean is divided into several oceanographic zones by a series of deep-reaching fronts (e.g. Orsi et al., 1995). These fronts, empirically linked to contours of sea surface height (SSH) (Sokolov and Rintoul, 2002, 2009a, 2009b), account for most of the water transport in the Southern Ocean (Nowlin and Clifford, 1982; Rintoul and Trull, 2001). Between the fronts lie zones of weak flow and relatively homogeneous water properties. From north to south these fronts and zones are the Subtropical Front (STF), the Subantarctic Zone (SAZ), the Subantarctic Front (SAF), the Polar Frontal Zone (PFZ) the Polar Front (PF), the Antarctic Zone (AZ) and the Southern Antarctic Circumpolar Current Front (SACCF) (Fig. 1; Orsi et al., 1995; Sokolov and Rintoul, 2002, 2009a). In the region south of Tasmania, the fronts are more tightly grouped than in other sectors, due to the presence of the bathymetric ridges to the north and south of the ACC (Chaigneau and Morrow, 2002; Sokolov and Rintoul, 2002) (Fig. 1). The STF represents the boundary between the warm and salty waters of the subtropical gyres to the north and the colder and fresher Antarctic Intermediate and Subantarctic Mode Waters of the SAZ to the south (AAIW and SAMW, respectively) (McCartney, 1977). The SAF, which is found around 51°S, is the strongest front of the Southern Ocean and main jet of the ACC. This front represents the limit between the waters of the SAZ and the PFZ (Fig. 1).

The SAZ and PFZ waters south of Tasmania exhibit HNLC characteristics but with important differences between them. In the PFZ, concentrations of phosphate, nitrate and silicate remain high until at least midsummer. In contrast, the surface waters of the SAZ exhibit low silicate concentrations throughout the year (Rintoul and Trull, 2001; Trull et al., 2001b; Bowie et al., 2011) (Fig. 1a). Moreover, the two regions exhibit different physical properties that influence primary production. The winter mixed layer in the SAZ can exceed 400 m depth, whereas in the PFZ it is typically shallower than 200 m (Rintoul and Trull, 2001). Both regions are Fe limited, but with variations in the seasonality of Fe delivery, with winter mixing dominating the supply of Fe to the PFZ, whereas this supply is augmented by greater aerosol and shelf Fe inputs throughout the year in the SAZ (Bowie et al., 2009). As a result of these different chemical and physical characteristics, both zonal systems exhibit two quite different phytoplankton production regimes. SAZ waters south of Tasmania are dominated by pico- and nanoplankton, including coccolithophores, cyanobacteria, autotrophic flagellates and lower abundances of diatoms. In contrast, the PFZ waters exhibit more diatoms, as well as, coccolithophores, flagellates but low abundance of cyanobacteria (Deacon, 1982; Wright et al., 1996; Popp et al., 1999; Kopczynska et al., 2001; de Salas et al., 2011).

### 2.2. Sediment trap moorings and core tops

Sediment trap moorings were deployed at two sites in the Southern Ocean along the 140°E meridian: the 47°S site located in the abyssal plain within the central SAZ (47°S, 142°E) and the 54°S site situated on a local bathymetric high of the Southeast Indian Ridge in the PFZ (54°S, 142°E) (Fig. 1, Table 1). These deployments were part of the

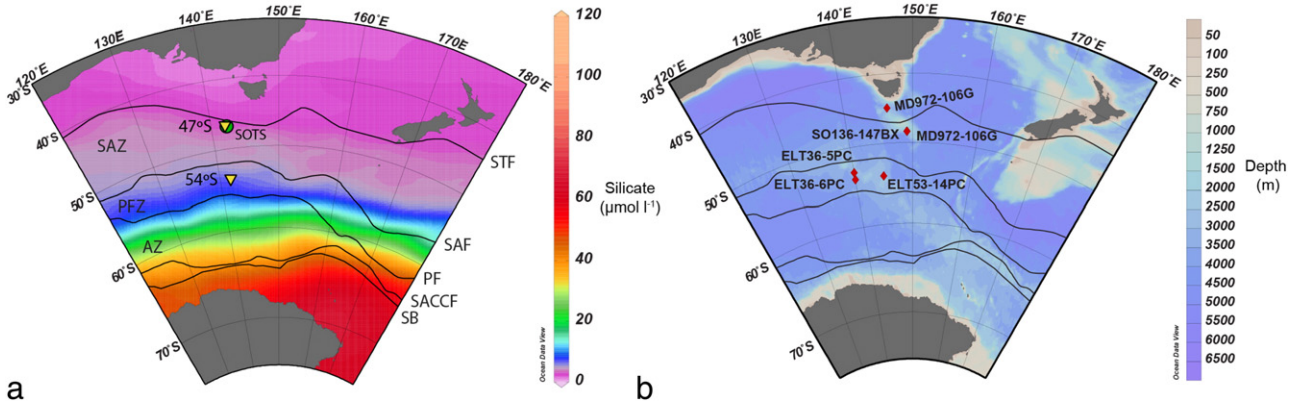


**Fig. 1.** a. Map of the SAZ project sediment trap mooring locations in relation to annual surface ocean silicate concentrations (Garcia et al., 2014). Sediment trap mooring locations 47°S, 54°S and 61°S are represented with yellow triangles and the Southern Ocean Time Series (SOTS) site with a green circle. b. Bathymetric map showing the location of the core tops (red diamonds) analyzed in this study. Core tops are as follows: 1, ELT36-5PC; 2, ELT53-14PC; 3, ELT36-6PC; 4, SO136-147BX; 5, MD972-108BX; 6, MD972-106G. GC refers to gravity core, BX to box core and PC to piston core. Abbreviations: STF – Subtropical Front, SAZ – Subantarctic Zone, SAF – Subantarctic Front, PFZ – Polar Frontal Zone, PF – Polar Front, AZ – Antarctic Zone, SACCF – Southern ACC Front and SB – Southern Boundary. Water masses and oceanic fronts from Orsi et al. (1995). (For interpretation of the references to colour in this figure legend, the reader is referred to the web version of this article.)

Australian SAZ project (Trull et al., 2001c). The mooring deployed at the 47°S site consisted of three automated McLane Parflux time-series sediment traps (21 cups) attached to a mooring line at approximately 1000, 2000 and 3800 m depth. The mooring deployed at the 54°S site had two sediment traps placed at 800 and 1500 m. The seafloor depth at the 47°S site is approximately 4500 m and at the 54°S, 2300 m. Thus the deepest traps were ~700 m above bottom at both locations. The two stations were occupied quasi-continuously for the decade 1997–2007. Biogenic flux data for the first year deployment 1997–98 can be found in Trull et al. (2001a), whereas biogenic particle and diatom assemblage composition registered by the shallower traps at the 47°S site (1000 m) between 1999–2001 and at the 54°S site (800 m) during six-selected years from 1997–2007 have been published by Rigual-Hernández et al. (2015b).

Here, we present biogeochemical and diatom species fluxes of the deep traps at the 47°S site (2000 and 3800 m) for the period 1999–2000 and at the 54°S station for the periods 1997–1998, 1999–2000 and 2003–2004. In addition, the diatom assemblages from six nearby core top sites (Fig. 1b, Table 2) were analyzed for comparison to sediment trap assemblages. Core tops were recovered from RV *Marion Dufresne* cruise 972 (MD972), RV *Sonne* cruise 136 (SO136) and RV *Eltanin* cruises 36 and 53 (ELT36 and ELT53).

### 2.3. 2.2 determination of major constituents of the flux

The splitting procedure and chemical analyses of the <1 mm fraction were carried out following the methodology described by Bray et al. (2000); Trull et al. (2001a) and Rigual-Hernández et al. (2015b). A total of 105 samples were processed for chemical analysis. Component fluxes for individual cups over the collection period are provided in Table 3. As the collection periods were shorter than a calendar year, annual mean estimates were determined and are presented in Table 4. These annual estimates take into consideration that unobserved days occurred during the winter months when fluxes were low, therefore the flux for the last winter cup was used to represent mean daily fluxes during the unobserved period. For small gaps (i.e. 1–2 cups) between samples outside the winter period, geochemical and diatom valve fluxes were estimated by linear interpolation between the preceding and succeeding cups.

### 2.4. Siliceous microplankton sample preparation

A total of 91 sediment trap samples and six surface sediment samples were processed for siliceous microplankton analysis. For diatom analysis a 1/10 split of the original sediment trap samples and 0.1–0.5 g of each core top were processed. Each split was refilled with distilled water to 40 ml, from which 10 ml was subsampled and buffered with a solution of sodium carbonate and sodium hydrogen carbonate (pH 8) and stored at 4 °C in the dark for future calcareous nannoplankton analysis. The remaining 30 ml was treated with potassium permanganate, hydrogen peroxide, and concentrated hydrochloric acid following the methodology used by Rigual-Hernández et al. (2015a). The core top sediment samples were rinsed with distilled water and prepared with the same methodology used for the sediment trap

**Table 1**
Summary table of SAZ project mooring stations, showing location, bottom depth, trap depth, deployment time and measured currents.

| Site and trap depths | Deployment | Deployment time | | Latitude | Longitude | Bottom depth m | Mean current speed cm $s^{-1}$ | Maximum current speed cm $s^{-1}$ |
|---|---|---|---|---|---|---|---|---|
| | | Start | End | °S | °E | | | |
| 54°S (PFZ) | 1997–1998 | | | 53°45′ | 141°45′ | 2280 | | |
| 800 m | | September 26, 1997 | February 17, 1998 | | | | 8.3 | 22.6 |
| 1500 m | | September 26, 1997 | February 17, 1998 | | | | 4.8 | 18.5 |
| 54°S (PFZ) | 1999–2000 | | | 53°45′ | 141°45′ | 2475 | | |
| 800 m | | July 21, 1999 | August 29, 2000 | | | | 10.0 | 24.0 |
| 1500 m | | July 21, 2000 | August 29, 2000 | | | | 5.0 | 20.0 |
| 54°S (PFZ) | 2003–2004 | | | 53°44′ | 141°45′ | 2205 | | |
| 800 m | | September 27, 2003 | October 09, 2004 | | | | 9.0 | 20.0 |
| 1500 m | | September 27, 2003 | October 09, 2004 | | | | – | – |
| 47°S (SAZ) | 1999–2000 | | | 46°47′ | 142°6′ | 4400 | | |
| 1000 m | | July 21, 1999 | August 29, 2000 | | | | 6.03 | 23 |
| 2000 m | | July 21, 1999 | August 29, 2000 | | | | – | – |
| 3800 m | | July 21, 1999 | August 29, 2000 | | | | 3.27 | 20 |

**Table 2**
Locations, depth and diatom valve concentration of the core tops recovered in the PFZ, SAZ and STS south of Australia along the ~140°E.

| Core top | Latitude (S) | Longitude (E) | Water depth (m) | Zonal system | Core depth (cm) | Diatoms (x $10^6$ valves/g) |
|---|---|---|---|---|---|---|
| ELT36-5 PC | 53°02′ | 139°59′ | 2963 | PFZ | 3–10 | 195 |
| ELT53-14 PC | 54°11.5′ | 144°57.2′ | 2186 | PFZ | 3–10 | 429 |
| ELT36-6 PC | 54°32.5′ | 140°03′ | 3356 | PFZ | 3–10 | 274 |
| SO136-147 BX | 48°29.99′ | 149°06.75′ | 2177 | SAZ | 0–2 | 1 |
| MD972-108 BX | 48°29.3′ | 149°6.3′ | 2140 | SAZ | 0–2 | 3 |
| MD972-106 GC | 45°9.69′ | 146°16.5′ | 3310 | STZ | 0–2 | 4 |

samples. Three replicate slides per sample were prepared following the standard decantation method outlined by Bárcena and Abrantes (1998). Qualitative and quantitative analyses were performed at ×400 and ×1000 magnification on an Olympus BH-2 compound light optical microscope with phase-contrast illumination. Several traverses across the cover-slip were examined, depending on diatom valve abundance. The resulting counts were converted into fluxes (in number $m^{-2}$ $d^{-1}$) according to Sancetta and Calvert (1988) and Romero et al. (2009). Relative abundances of diatom individual taxa are given as percentages of the total diatom assemblage in the traps and in the sediment. Concentrations of diatoms, silicoflagellates and radiolarians in the sediments are given as number of valves or skeletons in 1 g of dry sediment.

### 2.5. Taxonomic notes

Taxa were identified by light microscopy (LM) and scanning electron microscopy (SEM). Differentiation between *Pseudo-nitzschia lineola* and *Pseudo-nitzschia turgiduloides* was often difficult due to their poor preservation in the samples. Therefore, these two species were grouped under the category *Pseudo-nitzschia* cf. *lineola* in this study. The resting spores *Chaetoceros* (*Hyalochaete*) were identified only at group level. The *Thalassiosira trifulta* group includes all small *Thalassiosira* specimens with similar morphological features that fit within the description provided by Shiono and Koizumi (2000), i.e. inward tubes of the fultoportulae and a rimoportula located away from the valve margin. The varieties of *Thalassiosira gracilis* were grouped together under the category of *T. gracilis* following the recommendations of Crosta et al. (2005) and Fryxell (1994).

### 2.6. Particle settling velocities

The estimated sinking rates for the diatom assemblages at the meso- and bathypelagic depths of the PFZ and SAZ were calculated from the time lag between associated peaks of BSi and diatom species and the vertical distance between traps. The estimation of the settling velocities was only possible for the particle high flux period at both sites when distinct peaks were identified at different depths (Fig. 2). The precision of the calculation is limited by the duration of the sampling interval (8.5 to 14 days).

### 2.7. Efficiency of the sediment traps

Average ocean current speeds near trap depths during the deployments were <6 cm $s^{-1}$ at 1000 and 3800 m at the 47°S site and ≤10 cm $s^{-1}$ at 800 and 1500 m at the 54°S. These values are similar to those reported by Trull et al. (2001a) for the first year deployment and below the threshold above which significant hydrodynamic effects on trap collections are observed in conical sediment traps (12–15 cm $s^{-1}$; Baker et al., 1988; Gardner, 1989), although episodes of higher velocities did occur (Table 1). In order to constrain further the trapping efficiency of the traps, Trull et al. (2001a) compared the intercepted flux of $^{230}Th_{ex}$ to its production in the water column above the trap (Bacon, 1996; Yu et al., 2001). These results showed that the trapping efficiencies were very similar between the 47°S and 54°S stations and almost identical in the traps vertically moored at the same site (Trull et al., 2001a). Taken together, the above-mentioned observations suggest that the SAZ and PFZ sediment traps can be compared on an equal basis, with trap collection efficiencies representing only a minor aspect of latitudinal flux variations.

## 3. Results

### 3.1. Annual export fluxes

Flux data at stations 54°S and 47°S are listed in Table 3 and include fluxes at all depths for total particle, biogenic silica, carbonate, particulate organic carbon (POC) and diatom valves. Total and major component mass fluxes decreased between the 800 and 1500 m traps at the 54°S site. The mean annual fluxes of total mass, BSi, $CaCO_3$ and POC at this site decreased by a factor of 0.8, 0.8, 0.7 and 0.6, respectively (Table 4). Moreover, the BSi:POC ratio increased by a factor of 1.4 ± 0.0 (annual average ± one standard deviation) between the lower (800 m) and deeper (1500 m) traps. At the 47°S site, total mass flux decreased between 2000 and 3800 m but the shallowest trap (1000 m) exhibited lower fluxes than the two deep traps (Fig. 3 and Table 4). All the major chemical compounds followed a similar trend, with the exception of POC, which showed a decreasing trend with increasing depth with 1.1 g $m^{-2}$ $yr^{-1}$ at 1000 m, 0.9 g $m^{-2}$ $yr^{-1}$ at 2000 m and 0.5 g $m^{-2}$ $yr^{-1}$ at 3800 m (Fig. 3 and Table 4).

Biogenic silica was the largest component of the total mass flux at 54°S but contributed much less to the particle export at the 47°S site, which was dominated by carbonate. Furthermore, the increase of the BSi:POC ratios between 1000 and 2000 m and between 1000 and 3800 m were identical, 2.0 (annual value), because no change in BSi:POC occurred between the two deeper traps.

### 3.2. Seasonal variability of export fluxes

Maximum fluxes were registered during the summer months at the 54°S site and during spring and summer at the 47°S site. The fluxes of all the individual component fluxes at the 54°S site were closely correlated at both depths. The correlation between diatom valve and BSi fluxes was relatively weak at both depths (0.55 and 0.53 at 800 and 1500 m, respectively). These low correlation values were most likely due to the high fragmentation of the diatom valves in the samples of the summer 1999–00 (Rigual-Hernández et al., 2015b). Diatom fragments cannot be enumerated with our counting technique, and therefore discrepancies between the measurement of the biogenic silica content and the diatom valve flux in a sample with a high degree of fragmentation is likely. The correlations found between diatom flux and all the individual biochemical flux components improved significantly when excluding the 1999–2000 data series (0.85 and 0.93 at 800 and 1500 m, respectively). In the 47°S traps, diatom valve fluxes exhibited a weaker correlation with the major components than those of the 54°S site.

At the 54°S site the total annual diatom flux in the shallower trap was lower than in the deeper sediment trap by a factor of 0.8. Thus, the increase of the diatom valve fluxes with depth lies within the range of total, biogenic silica, carbonate and POC variations (see above). In the SAZ, the diatom valve flux export follows the same

**Table 3**
Individual cup fluxes for <1 mm fraction of total mass, biogenic silica, calcium carbonate, particulate organic carbon (POC) and diatom valves at trap sites (a) 47°S (1000, 2000 and 3800 m) from July 1999 to August 2000 and (b) 54°S (800 and 1500 m) from September 1997 to February 1998, July 1999 to August 2001 and September 2003 to October 2005.

a

| Deployment | Cup number | Date mid-point | Length days | Total mass mg $m^{-2}$ $d^{-1}$ | | | $BSiO_2$ mg $m^{-2}$ $d^{-1}$ | | | $CaCO_3$ mg $m^{-2}$ $d^{-1}$ | | | POC mg $m^{-2}$ $d^{-1}$ | | | Diatoms $10^6$ valves $m^{-2}$ $d^{-1}$ | | |
|---|---|---|---|---|---|---|---|---|---|---|---|---|---|---|---|---|---|---|
| | | | | 1000 m | 2000 m | 3800 m | 1000 m | 2000 m | 3800 m | 1000 m | 2000 m | 3800 m | 1000 m | 2000 m | 3800 m | 1000 m | 2000 m | 3800 m |
| 47°S | 1 | 31/07/1999 | 20.0 | 19.6 | 18.8 | 17.9 | 0.8 | 1.0 | 0.5 | 8.6 | 12 | 13.3 | 3.0 | 1.3 | 0.7 | 0.002 | 0.057 | 0.069 |
| 1999–2000 | 2 | 20/08/1999 | 20.0 | 27.1 | 35.0 | 29.5 | 3.4 | 2.1 | 1.2 | 15.3 | 24 | 24.6 | 2.8 | 2.0 | 0.8 | 0.113 | 0.173 | 0.057 |
| | 3 | 06/09/1999 | 15.0 | 45.9 | 40.2 | 35.8 | 5.1 | 3.4 | 1.5 | 26.2 | 30 | 27.3 | 4.2 | 2.1 | 1.7 | 0.195 | 0.213 | 0.176 |
| | 4 | 21/09/1999 | 15.0 | 57.5 | 49.9 | 47.8 | 5.4 | 5.0 | 2.6 | 36.0 | 37 | 35.3 | 4.4 | 2.1 | 1.7 | 0.147 | 0.234 | 0.227 |
| | 5 | 04/10/1999 | 10.0 | 66.5 | 46.5 | 47.5 | 7.9 | 3.8 | 2.5 | 46.8 | 35 | 37.8 | 4.2 | 2.2 | 1.3 | 0.213 | 0.131 | 0.250 |
| | 6 | 14/10/1999 | 10.0 | 65.9 | 38.1 | 29.0 | 3.8 | 2.8 | 1.7 | 46.1 | 28 | 23.4 | 4.2 | 2.0 | 0.8 | 0.364 | 0.159 | 0.067 |
| | 7 | 24/10/1999 | 10.0 | 89.8 | 53.6 | 41.3 | 4.3 | 3.2 | 2.6 | 66.4 | 41 | 33.1 | 5.3 | 2.3 | 1.3 | 0.137 | 0.281 | 0.253 |
| | 8 | 03/11/1999 | 10.0 | 73.9 | 72.5 | 45.5 | 3.8 | 4.4 | 2.4 | 56.9 | 58 | 36.8 | 4.1 | 3.0 | 1.3 | 0.080 | 0.272 | 0.419 |
| | 9 | 13/11/1999 | 10.0 | 12.7 | 64.4 | 37.4 | 0.2 | 4.5 | 1.9 | 9.1* | 53 | 30.6 | 1.1* | 2.2 | 1.1 | | 0.305 | 0.268 |
| | 10 | 23/11/1999 | 10.0 | 4.2 | 60.6 | 42.6 | 0.2* | 7.0 | 2.3 | 3.0* | 50 | 34.5 | 0.5* | 2.0 | 1.1 | | 0.350 | 0.186 |
| | 11 | 03/12/1999 | 10.0 | 4.3 | 46.4 | 21.5 | 0.2* | 3.0 | 1.1 | 3.1* | 37 | 17.9 | 0.5* | 1.7 | 0.6 | | 0.273 | 0.099 |
| | 12 | 13/12/1999 | 10.0 | 13.8 | 47.6 | 21.7 | 0.8* | 3.9 | 1.4 | 9.9* | 39 | 20.3 | 2.0* | 1.5 | 0.3 | | 0.180 | 0.098 |
| | 13 | 23/12/1999 | 10.0 | 32.6 | 54.7 | 36.4 | 2.4 | 6.0 | 2.8 | 19.3 | 40 | 29.9 | 3.7 | 2.0 | 0.8 | 0.049 | 0.202 | 0.252 |
| | 14 | 02/01/2000 | 10.0 | 38.5 | 51.3 | 70.2 | 2.2 | 5.4 | 5.2 | 25.0 | 38 | 57.4 | 3.6 | 2.1 | 1.7 | 0.001 | 0.223 | 0.341 |
| | 15 | 12/01/2000 | 10.0 | 15.9 | 59.8 | 40.2 | 0.1 | 6.4 | 2.4 | 9.5* | 44 | 32.6 | 1.9* | 2.4 | 1.2 | | 0.204 | 0.102 |
| | 16 | 22/01/2000 | 10.0 | 14.0 | 64.5 | 34.6 | 0.6 | 8.8 | 2.1* | 8.4* | 47 | 27.1* | 1.6* | 2.6 | 1.4* | | 0.822 | |
| | 17 | 03/02/2000 | 15.0 | 11.4 | 45.6 | 30.9 | 0.2 | 5.7 | 1.9 | 6.8* | 31 | 23.5 | 1.1* | 2.6 | 1.5 | 0.002 | 0.286 | 0.068 |
| | 18 | 21/02/2000 | 20.0 | 8.0 | 24.8 | 52.4 | 0.0 | 2.2 | 3.7* | 4.8* | 15 | 40.5* | 1.0* | 2.1 | 2.7* | | | |
| | 19 | 01/04/2000 | 60.0 | 39.6 | 58.3 | 57.8 | 2.9 | 5.4 | 4.1 | 23.4 | 37 | 44.8* | 4.7 | 4.7 | 2.9* | 0.110 | 0.142 | |
| | 20 | 31/05/2000 | 60.0 | 47.0 | 44.2 | 48.5 | 5.1 | 4.2 | 3.5 | 33.2 | 35 | 37.5 | 3.3 | 1.7 | 1.5 | 0.125 | 0.309 | 0.157 |
| | 21 | 30/07/2000 | 60.0 | 13.0 | 52.4 | 23.9 | 0.7 | 3.4 | 1.5 | 7.4 | 39 | 19.3 | 1.6 | 2.2 | 0.7 | 0.002 | 0.273 | 0.102 |

b

| Deployment | Cup | Date mid-point | Length days | Total Mass mg $m^{-2}$ $d^{-1}$ | | $BSiO_2$ mg $m^{-2}$ $d^{-1}$ | | $CaCO_3$ mg $m^{-2}$ $d^{-1}$ | | POC mg $m^{-2}$ $d^{-1}$ | | Diatoms $10^6$ valves $m^{-2}$ $d^{-1}$ | |
|---|---|---|---|---|---|---|---|---|---|---|---|---|---|
| | | | | 800 m | 1500 m | 800 m | 1500 m | 800 m | 1500 m | 800 m | 1500 m | 800 m | 1500 m |
| 54°S | 1 | 26/09/1997 | 8.5 | 3 | 21 | 1* | 11 | 1 | 5 | 0* | 1 | 0.275 | 2.078 |
| 1997–1998 | 2 | 04/10/1997 | 8.5 | 12 | 21 | 6* | 11 | 3 | 5 | 0* | 1 | | 2.078 |
| | 3 | 13/10/1997 | 8.5 | 12 | 31 | 6* | 15 | 3 | 9 | 0* | 1 | | 2.585 |
| | 4 | 21/10/1997 | 8.5 | 47 | 31 | 25 | 15 | 13 | 9 | 1 | 1 | 4.561 | 2.585 |
| | 5 | 30/10/1997 | 8.5 | 100 | 39 | 53 | 21 | 26 | 11 | 3 | 1 | 13.121 | 2.121 |
| | 6 | 07/11/1997 | 8.5 | 142 | 71 | 79 | 35 | 36 | 19 | 2 | 1 | 20.564 | 7.812 |
| | 7 | 16/11/1997 | 8.5 | 233 | 93 | 132 | 50 | 56 | 24 | 4 | 2 | 26.211 | 6.952 |
| | 8 | 24/11/1997 | 8.5 | 166 | 129 | 82 | 69 | 46 | 32 | 4 | 3 | 11.542 | 17.069 |
| | 9 | 03/12/1997 | 8.5 | 53 | 135 | 13 | 62 | 21 | 46 | 2 | 2 | 4.914 | 15.364 |
| | 10 | 11/12/1997 | 8.5 | 63 | 184 | 21 | 107 | 17 | 43 | 2 | 3 | | 32.577 |
| | 11 | 20/12/1997 | 8.5 | 148 | 252 | 64 | 156 | 27 | 44 | 5 | 5 | 11.711 | 41.101 |
| | 12 | 28/12/1997 | 8.5 | 112 | 153 | 39 | 87 | 30 | 27 | 5 | 4 | 20.881 | 39.802 |
| | 13 | 04/01/1998 | 4.3 | 110 | 85 | 51 | 49 | 29 | 16 | 5 | 3 | 34.729 | 14.090 |
| | 14 | 08/01/1998 | 4.3 | 100 | 92 | 54 | 54 | 23 | 16 | 5 | 3 | | 22.598 |
| | 15 | 12/01/1998 | 4.3 | 152 | 131 | 93 | 78 | 29 | 18 | 4 | 4 | | 34.662 |
| | 16 | 16/01/1998 | 4.3 | 153 | 84 | 88 | 50 | 31 | 12 | 6 | 3 | | 37.260 |
| | 17 | 21/01/1998 | 4.3 | 265 | 81 | 165 | 34 | 51 | 13 | 9 | 2 | 70.808 | 21.129 |
| | 18 | 25/01/1998 | 4.3 | 396 | 116 | 259 | 75 | 66 | 15 | 10 | 3 | 54.059 | 23.949 |
| | 19 | 31/01/1998 | 8.5 | 276 | 81 | 172 | 49 | 47 | 11 | 7 | 2 | 41.101 | 33.400 |
| | 20 | 09/02/1998 | 8.5 | 142 | 47 | 74 | 31 | 37 | 6 | 5 | 1 | 28.947 | 24.436 |
| | 21 | 17/02/1998 | 8.5 | 66 | 34 | 30 | 21 | 20 | 5 | 2 | 1 | | 8.288 |
| 1999–2000 | 1 | 31/07/1999 | 20 | 46 | 102 | 34 | 69 | 2 | 4 | 1 | 1 | 9.681 | 7.647 |
| | 2 | 20/08/1999 | 20 | 72 | 60 | 53 | 42 | 3 | 4 | 1 | 1 | 10.944 | 7.935 |
| | 3 | 06/09/1999 | 15 | 81 | 78 | 63 | 57 | 4 | 5 | 1 | 1 | 7.948 | 7.243 |
| | 4 | 21/09/1999 | 15 | 25 | 51 | 17 | 36 | 3 | 5 | 1 | 1 | 4.867 | 4.026 |
| | 5 | 04/10/1999 | 10 | 45 | 13 | 32 | 7 | 3 | 2 | 1 | 1 | 5.622 | |
| | 6 | 14/10/1999 | 10 | 101 | 57 | 71 | 35 | 6 | 6 | 1 | 1 | 9.942 | 10.477 |
| | 7 | 24/10/1999 | 10 | 58 | 44 | 38 | 27 | 6 | 4 | 1 | 1 | 8.689 | 7.516 |
| | 8 | 03/11/1999 | 10 | 106 | 28 | 62 | 24 | 11 | 3 | 4 | 0 | 5.857 | 9.566 |
| | 9 | 13/11/1999 | 10 | 122 | 17 | 80 | 9 | 20 | 3 | 3 | 0 | 6.081 | 1.479 |
| | 10 | 23/11/1999 | 10 | 294 | 44 | 171 | 22 | 64 | 10 | 7 | 1 | 28.312 | 6.828 |
| | 11 | 03/12/1999 | 10 | 515 | 64 | 302 | 31 | 108 | 14 | 17 | 2 | 51.610 | 3.410 |
| | 12 | 13/12/1999 | 10 | 724 | 175 | 429 | 90 | 142 | 36 | 23 | 6 | 10.590 | 23.447 |
| | 13 | 23/12/1999 | 10 | 661 | 525 | 396 | 292 | 106 | 96 | 20 | 10 | 15.287 | 32.913 |
| | 14 | 02/01/2000 | 10 | 511 | 1039 | 309 | 630 | 58 | 141.9 | 16 | 20.15 | 19.142 | 56.081 |
| | 15 | 12/01/2000 | 10 | 339 | 773 | 207 | 475 | 36 | 100.3 | 10 | 14.87 | 17.274 | 36.361 |
| | 16 | 22/01/2000 | 10 | 11 | 270 | 6 | 172 | 2 | 50 | 0 | 5 | | 11.588 |

(continued on next page)

**Table 3** (*continued*)

b

| Deployment | Cup | Date mid-point | Length days | Total Mass mg $m^{-2}$ $d^{-1}$ | | $BSiO_2$ mg $m^{-2}$ $d^{-1}$ | | $CaCO_3$ mg $m^{-2}$ $d^{-1}$ | | POC mg $m^{-2}$ $d^{-1}$ | | Diatoms $10^6$ valves $m^{-2}$ $d^{-1}$ | |
|---|---|---|---|---|---|---|---|---|---|---|---|---|---|
| | | | | 800 m | 1500 m | 800 m | 1500 m | 800 m | 1500 m | 800 m | 1500 m | 800 m | 1500 m |
| | 17 | 03/02/2000 | 15 | 104 | 41 | 36 | 21 | 52 | 6 | 3 | 2 | 3.892 | 13.426 |
| | 18 | 21/02/2000 | 20 | 194 | 12 | 119 | 7 | 34 | 2 | 4 | 0 | 11.224 | 4.967 |
| | 19 | 01/04/2000 | 60 | 132 | 0 | 69 | 0* | 29 | 0* | 3 | 0* | 4.764 | |
| | 20 | 31/05/2000 | 60 | 50 | 7 | 31 | 4 | 6 | 1 | 1 | 0 | 3.390 | 3.852 |
| | 21 | 30/07/2000 | 60 | 37 | 0 | 20 | 0* | 5 | 0* | 1 | 0* | 1.117 | |
| 2003–2004 | 1 | 10/4/2003 | 14 | 15 | 19 | 8* | 13 | 5* | 3 | 1* | 0 | 0.352 | 4.504 |
| | 2 | 10/18/2003 | 14 | 23 | 30 | 13 | 16 | 7 | 7 | 1 | 2 | 1.143 | 3.042 |
| | 3 | 11/1/2003 | 14 | 35 | 26 | 19 | 13 | 11 | 10 | 1 | 1 | 2.808 | 1.870 |
| | 4 | 11/15/2003 | 14 | 121 | 47 | 55 | 21 | 20 | 13 | 2 | 1 | 11.519 | 6.519 |
| | 5 | 11/29/2003 | 14 | 76 | 55 | 36 | 25 | 15 | 13 | 2 | 1 | 7.748 | 6.114 |
| | 6 | 12/13/2003 | 14 | 179 | 84 | 112 | 45 | 40 | 23 | 4 | 2 | 19.892 | 14.083 |
| | 7 | 12/27/2003 | 14 | 233 | 227 | 135 | 138 | 44 | 46 | 7 | 7 | 10.320 | 43.198 |
| | 8 | 1/10/2004 | 14 | 182 | 284 | 114 | 190 | 34 | 53 | 6 | 6 | 30.998 | 124.482 |
| | 9 | 1/24/2004 | 14 | 122 | 235 | 82 | 167 | 21 | 29 | 3 | 5 | 16.786 | 97.337 |
| | 10 | 2/7/2004 | 14 | 64 | 127 | 37 | 91 | 11 | 12 | 3 | 3 | 11.142 | 50.809 |
| | 11 | 2/21/2004 | 14 | 29 | 161 | 17 | 105 | 7 | 20 | 1 | 3 | 5.982 | 60.824 |
| | 12 | 3/6/2004 | 14 | 31 | 1 | 18 | 1 | 8 | 0 | 1 | 0 | 6.189 | 0.055 |
| | 13 | 3/20/2004 | 14 | 66 | 3 | 45 | 2 | 10 | 0 | 1 | 0 | 9.824 | 0.629 |
| | 14 | 4/3/2004 | 14 | 85 | 1 | 53 | 0 | 17 | 0 | 1 | 0 | 11.515 | 0.025 |
| | 15 | 4/17/2004 | 14 | 16 | 0 | 10 | 0 | 5 | 0 | 1 | 0 | 0.622 | |
| | 16 | 5/1/2004 | 14 | 11 | 0 | 7 | 0 | 4 | 0 | 0 | 0 | 0.658 | |
| | 17 | 5/25/2004 | 35 | 20 | 0 | 14 | 0 | 3 | 0 | 0 | 0 | 3.431 | |
| | 18 | 6/29/2004 | 35 | 19 | 1 | 11 | 0 | 4 | 0 | 1 | 0 | 1.549 | 0.022 |
| | 19 | 8/3/2004 | 35 | 14 | 0 | 6 | 0 | 3 | 0 | 2 | 0 | 1.235 | 0.014 |
| | 20 | 9/7/2004 | 35 | 10 | 0 | 5 | 0 | 4 | 0 | 1 | 0 | 1.088 | |
| | 21 | 10/2/2004 | 14 | 7 | 0 | 4 | 0 | 2 | 0 | 1 | 0 | 0.458 | |

* Component fluxes representing intervals for which insufficient material was available for component measurement and were estimated.

trend as that of BSi, increasing from 1000 to 2000 m and decreasing from 2000 to 3800 m.

### 3.3. Particle-settling velocity

Sinking rates during the productive period (approximately from November to January) ranged between 20 and 50 m $d^{-1}$ at the 54°S site. Settling velocities at the 47°S site were of 20 m $d^{-1}$ between 1000 m and 2000 m and 45 m $d^{-1}$ between 2000 m and 3800 m (October to January).

### 3.4. Diatom species fluxes

The composition and seasonal variability of the diatom sinking assemblages captured by the shallower traps at the 54°S and 47°S sites are described in detail in Rigual-Hernández et al. (2015b). The same species occurring at the shallower traps (Rigual-Hernández et al., 2015b) were indentified in the deeper traps (Fig. 4). At 1500 m in the 54°S trap, 10 species or species groups contributed to >90% of the total diatom assemblage. The annual diatom assemblage was dominated by *Fragilariopsis kerguelensis* (60%), followed by *Pseudo-nitzschia lineola* cf. *lineola* (10%), *Thalassiosira gracilis* (6%), *Pseudo-nitzschia heimii* (3.7%), *Fragilariopsis rhombica* (3%), *Thalassiosira lentiginosa* (2%), *Fragilariopsis pseudonana* (2%), *Navicula directa* (2%), *Thalassiosira* spp. <20 μm and *Chaetoceros dichaeta* (1%) (Fig. 4). At the 47°S site, the diatom assemblage was more diversified. *Fragilariopsis kerguelensis* also dominated the diatom assemblages at 2000 and 3800 m (48 and 45%, respectively), with subordinate contributions of *Azpeitia tabularis* (10 and 13%), *Thalassiosira* sp. 1 (3.9 and 4.4%), *Nitzschia bicapitata* (3.6 and 2.1%), *Chaetoceros* RS (3.5 and 5.3%), *Thalassiosira* spp. >20 μm

**Table 4**
Annual biogeochemical and total diatom valve fluxes at different depths for <1 mm fraction at the 47°S and 54°S sites.

(a) Annual fluxes of biogeochemical components (g $m^{-2}$ $y^{-1}$) and diatom valves (valves $10^8$ $m^{-2}$ $y^{-1}$) at the PFZ site (54°S).

| 54°S deployment | Depth (m) | Total mass flux g $m^{-2}$ $y^{-1}$ | $SiO_2$-bio g $m^{-2}$ $y^{-1}$ | % | PIC as $CaCO_3$ g $m^{-2}$ $y^{-1}$ | % | POC g $m^{-2}$ $y^{-1}$ | % | BSi:POC molar ratio | Diatom valves (×$10^8$) valves $m^{-2}$ $y^{-1}$ |
|---|---|---|---|---|---|---|---|---|---|---|
| 1997–1998 | 800 | 19 | 10.1 | 53 | 4.3 | 23 | 0.6 | 2.9 | 3.65 | 30.2 |
| | 1500 | 14 | 8.1 | 56 | 3.0 | 21 | 0.3 | 2.3 | 4.93 | 28.6 |
| 1999–2000 | 800 | 52 | 30.8 | 60 | 8.7 | 17 | 1.4 | 2.7 | 4.37 | 29.1 |
| | 1500 | 33 | 20.2 | 61 | 4.7 | 14 | 0.7 | 2.0 | 6.22 | 18.8 |
| 2003–2004 | 800 | 20 | 11.5 | 59 | 4.0 | 20 | 0.6 | 3.1 | 3.81 | 22.5 |
| | 1500 | 18 | 11.2 | 64 | 3.1 | 18 | 0.4 | 2.3 | 5.44 | 14.5 |

(b) Annual fluxes of biogeochemical components (g $m^{-2}$ $y^{-1}$) and diatom valves (valves $10^8$ $m^{-2}$ $y^{-1}$) at the SAZ site (47°S).

| 47°S deployment | Depth (m) | Total mass flux g $m^{-2}$ $y^{-1}$ | $SiO_2$-bio g $m^{-2}$ $y^{-1}$ | % | PIC as $CaCO_3$ g $m^{-2}$ $y^{-1}$ | % | POC g $m^{-2}$ $y^{-1}$ | % | BSi:POC molar ratio | Diatom valves (×$10^8$) valves $m^{-2}$ $y^{-1}$ |
|---|---|---|---|---|---|---|---|---|---|---|
| 1999–2000 | 1000 | 12 | 0.9 | 8 | 7.7 | 65 | 1.1 | 9.0 | 0.17 | 0.3 |
| | 2000 | 18 | 1.5 | 9 | 12.9 | 73 | 0.9 | 5.0 | 0.35 | 0.9 |
| | 3800 | 15 | 0.9 | 6 | 11.5 | 79 | 0.5 | 3.7 | 0.35 | 0.6 |

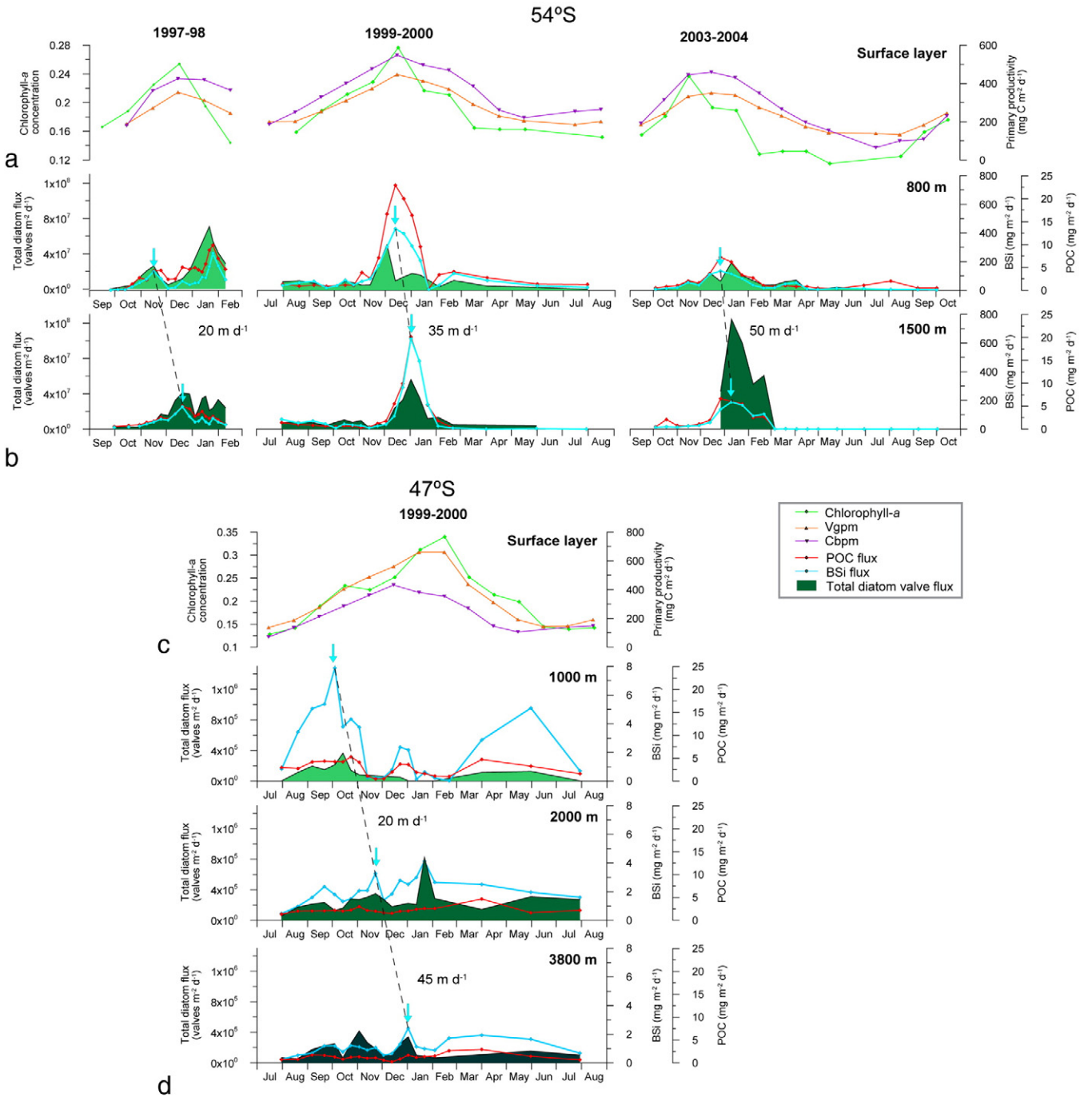


**Fig. 2.** Satellite-derived chlorophyll-*a* concentration and primary productivity estimates (standard vertically generalized production model – VGPM; and carbon-based production model – CbPM) for the surface layer at the 54°S and 47°S sites (a, c). Flux records for biogenic silica and total diatom valves at the 54°S site at 800 and 1500 m water depth (b) and at the 47°S at 1000, 2000, 3800 m depth (d). The solid arrows linked by dashed lines indicate associated peaks of biogenic silica fluxes at different depths used for estimating the settling rates.

(2.9 and 2.4%), *Thalassiosira* spp. <20 μm (2.6 and 2%) and *Hemidiscus cuneiformis* (2.5 and 3.6%).

Seasonally, the sinking diatom assemblages at the 54°S site were dominated by *F. kerguelensis* during the low-productive season (up to 96% from September to early November 1999). In contrast, the abundance of *F. kerguelensis* dropped during the high particle flux period (to below 25%) mainly due to the development of bloom-forming species such as by *P-n. lineola* cf. *lineola*, *T. gracilis*, *F. rhombica*, *F. pseudonana* and *N. directa*, i.e. the "high export group" sensu Rigual-Hernández et al. (2015b). At the 47°S site, the seasonality in the diatom assemblage composition was not as clearly expressed as in the 54°S site. *Fragilariopsis kerguelensis* exhibited a less pronounced seasonal variability with values ranging between 30–40%, with slightly higher values in the last cups of the record (up to 62% during the low productive season). Moreover, no remarkable increase in the relative contribution of members of the "high export group" was observed during the period of maximum export (i.e. spring and summer).

### 3.5. Diatom assemblages preserved in the surface sediments

The concentration of total diatom valves in the surface sediments closely follows the spatial trend observed in the sediment traps. Highest absolute contribution was seen in the PFZ (ELT53-14PC;

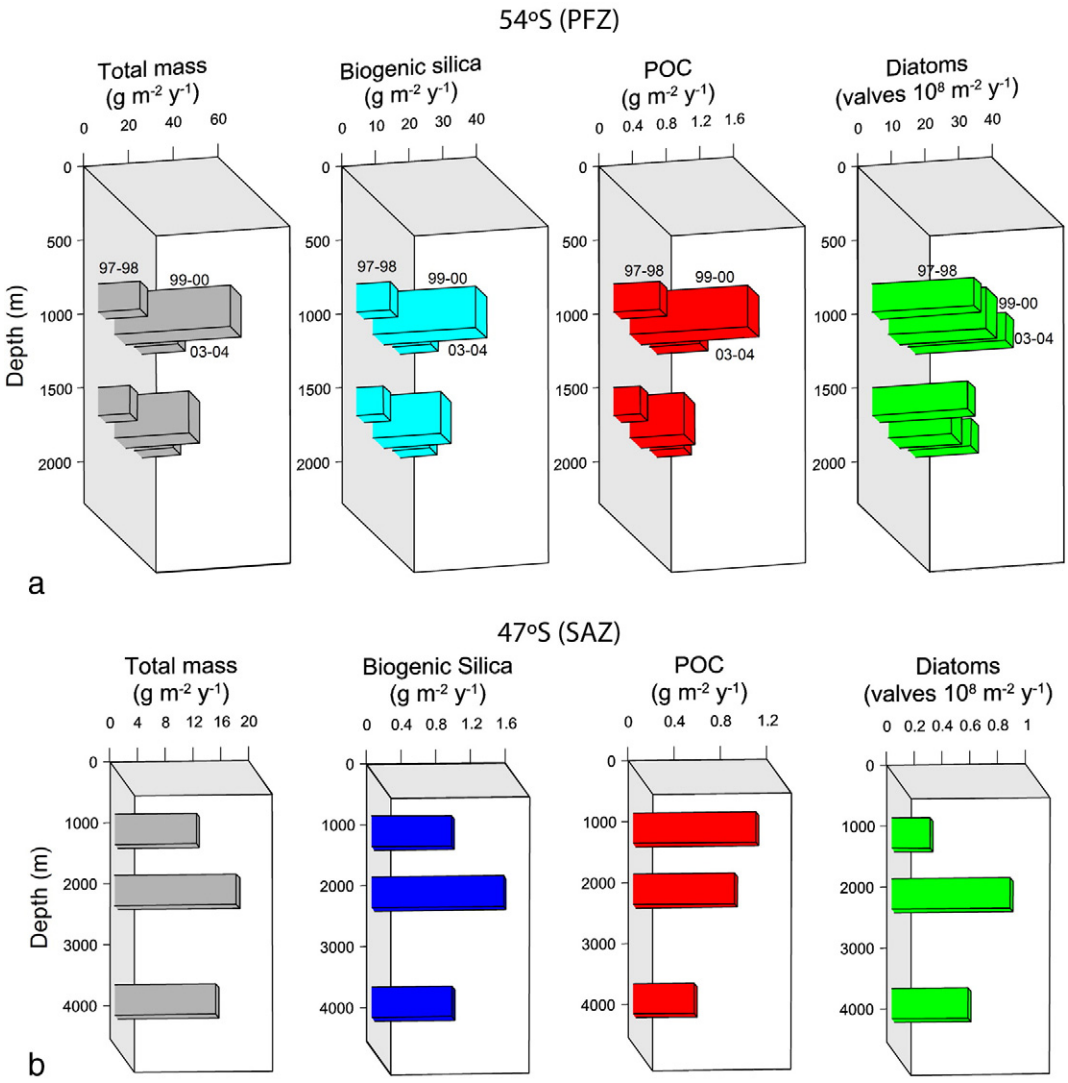


**Fig. 3.** Annual total and major component mass fluxes for the <1 mm particulate fraction at (a) 800 and 1500 m at the 54°S site for the periods 1997–98, 1999–2000 and 2003–04 and at (b) 1000, 2000 and 3800 m at the 47°S site for the period 1999–2000.

429 × $10^6$ valves $g^{-1}$) and lowest in the SAZ (MD972-108B −3 × $10^6$ valves $g^{-1}$; SO136-147BX 1 × $10^6$ valves $g^{-1}$) and Subtropical Zone (STZ) (MD972-106 4 × $10^6$ valves $g^{-1}$) (Table 3). Yet with respect to diatom species composition, significant discrepancies were observed between the trapped diatom assemblages and those preserved in the surface sediments. Overall, a strong increase in the relative contribution of the most robust diatom species was seen in the surface sediments. Within the PFZ, the heavily silicified *Fragilariopsis kerguelensis* increased its relative contribution from about ~60% in the 54°S traps, to up to ~90% in the underlying sediments (Fig. 4). In contrast, more weakly silicified diatoms, such as *Fragilariopsis pseudonana* and *Pseudo-nitzschia* species, (Fig. 4) which were important contributors to the diatom assemblages in the traps, were not preserved in the sedimentary record. Within the SAZ, an increase of the relative contribution of the more robust species (e.g. *F. kerguelensis* and *T. lentiginosa*) between the traps and sediments was also observed, although the increase was less pronounced than seen in the PFZ (Fig. 6).

## 4. Discussion

### 4.1. Annual flux

Overall, the magnitude of the total and major component mass fluxes measured by the deep traps were broadly in line with those previously reported for the first year deployment (1997–98) by Trull et al. (2001a). In the PFZ, the increasing factor of the BSi:POC ratio between trap depths (1.4) was somewhat less than the expectation of 1.7 (range 1.5 to 2.1) for POC flux attenuated according to a power law with expectation power exponent (commonly called the b-exponent) estimate of 0.86 (Martin et al., 1987) and range reflecting global ranges in b-exponents of 0.6 to 1.2 (Boyd and Trull, 2007) and negligible BSi remineralization (Nelson et al., 2002). Thus, the lower value suggests some accompanying remineralization of BSi between 800 and 1500 m in the PFZ. In the SAZ, the identical increasing ratios of BSi:POC ratios between 1000 and 2000 m and between 1000 and 3800 m (2.0) is consistent with the expectation that most remineralization is completed in

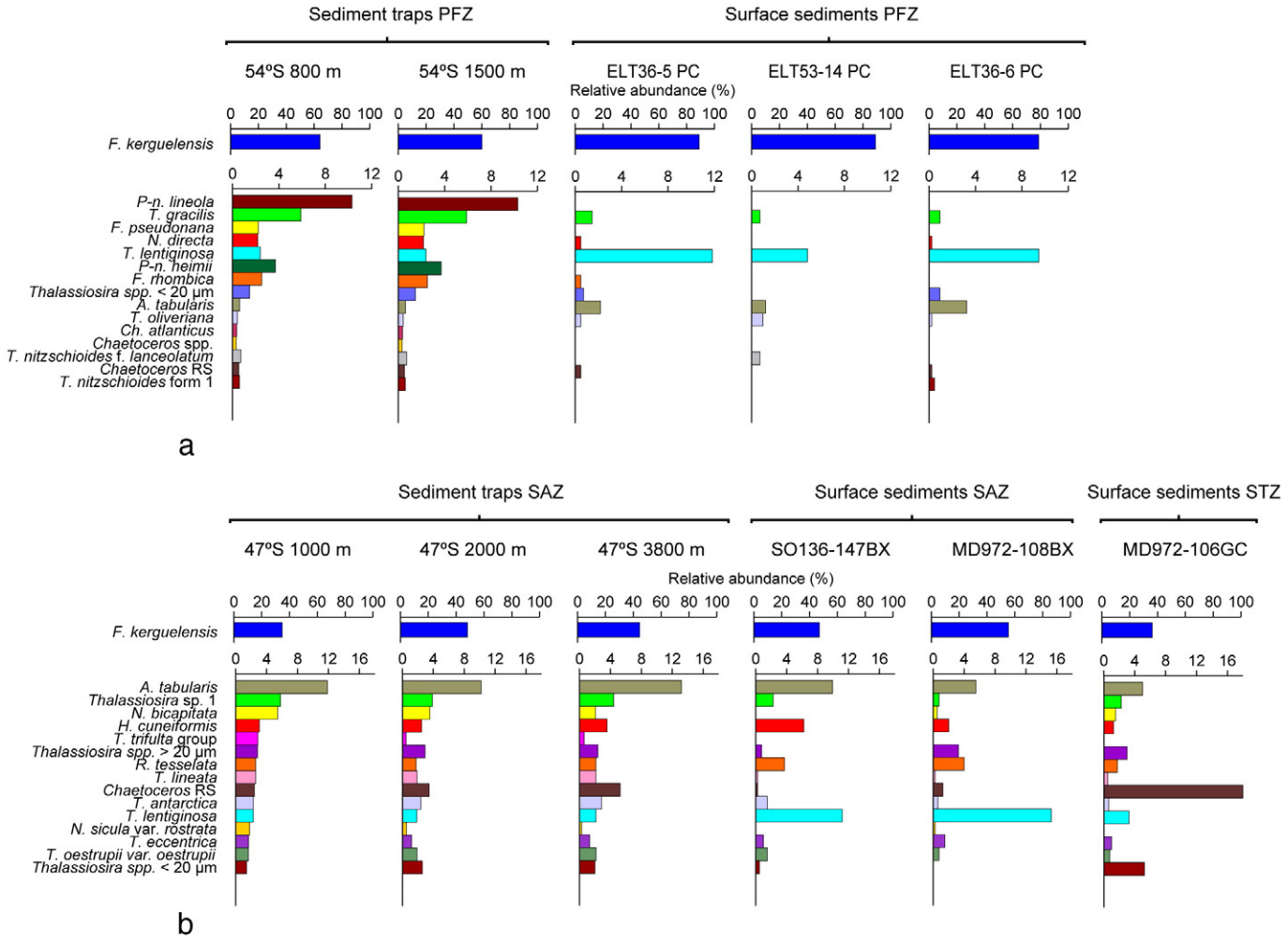


**Fig. 4.** Relative abundance of the most abundant diatom taxa collected at the 54°S site (800 and 1500 m) and surface sediments of the PFZ near the mooring location and (b) at the 47°S site (1000, 2000 and 3800 m) and surface sediments of the SAZ near the mooring location north of the STF.

the upper water column and at depth POC remineralization is tightly tied to mineral phase remineralization (Armstrong et al., 2002).

### 4.2. Diatom production and export to 1 km depth

Variations in the magnitude of particulate fluxes at the 54°S and 47°S sites were primarily driven by the seasonal cycle of primary production (Fig. 2). At the PFZ, monthly composites of chlorophyll-*a* concentration revealed a short, weak maximum from November to December (0.22–0.25 mg $m^{-3}$) during the three years studied. During the productive period of 1997–98 and 2003–04, a time lag of 1 month between the maximum biomass accumulation in the surface waters and maximum BSi, POC and diatom fluxes to the 800 m trap was observed (Fig. 2). The duration of this time lag is in line with findings in the Pacific sector by Buesseler et al. (2001) and in the Antarctic Zone (AZ) waters south of Tasmania by Rigual-Hernández et al. (2015a) who reported a similar offset between peak algal biomass accumulation in the surface and biogenic particle export. However, during the "growth season" of 1999–00, peak chlorophyll-*a* concentrations and primary productivity in the surface waters were concurrent with the maximum biogenic particle and diatom valve export (December 1999; Fig. 2). The temporal delay between production in the surface layer and export out of the mixed layer is considered influenced by the existing food web structure (e.g. Buesseler, 1998; Lutz et al., 2007). Indeed, recent findings by Laurenceau-Cornec et al. (in prep.) using a coupled physical-biogeochemical model with data from the Southern Ocean Time Series site (SOTS) (Fig. 1a) suggest that the longest delays between production and export are associated with blooms of small phytoplankton. In order to be exported from the surface layer, such small phytoplankton cells need to be either consumed by organisms at higher trophic levels or to form very large aggregates. Therefore, the delay between the production and export of small phytoplankton tends to be longer, i.e. a retention food web. Conversely, short time lags seem to be associated with large phytoplankton cells exported directly as algal aggregates, i.e. an export food web.

Although the estimation of the time lag between peak algal biomass accumulation in the surface waters and peak export pulses registered by the traps is fraught with uncertainties, the taxonomic analysis of the sinking diatom assemblages provides some insights that could help to explain the different time lags between production and export between years. During the 1999–00 high particle flux period, the relative contribution of the "high export group" (Rigual-Hernández et al., 2015b; see section 3.4) was remarkably higher compared with all other years (up to 64% of the total diatom assemblage in January; Fig. 5). All the components of the "high export group" are thought to undergo rapid cell division during favourable growth conditions giving rise to the formation of large and rapidly sinking aggregates that are responsible for the deepest flux (e.g. Assmy et al., 2007; Smetacek et al., 2012; Grigorov et al., 2014; Sackett et al., 2014). We speculate that rapid export during the summer of 1999–2000 was a result of massive growth in these boom-and-bust strategists. The fast growth rates of the species comprising the "high export group" most likely increased the potential of forming rapidly

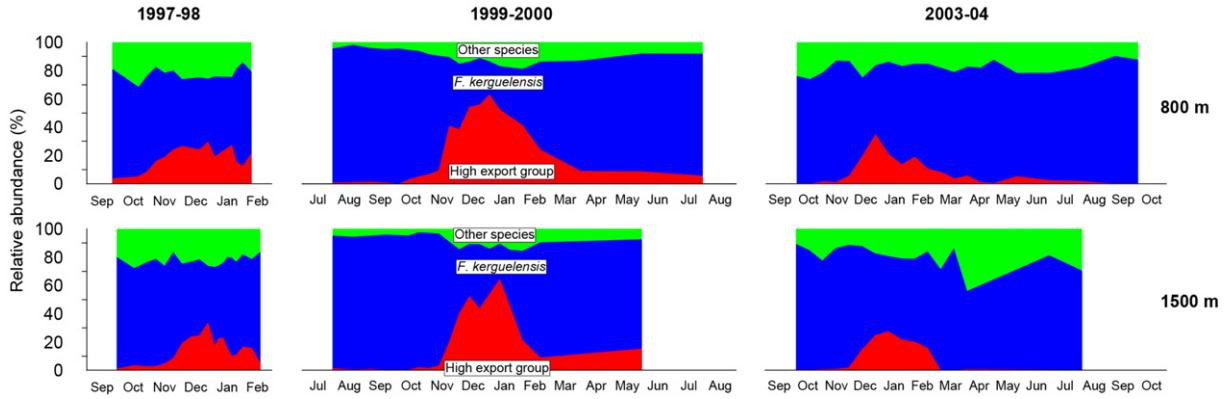


**Fig. 5.** Relative abundance of the "high export group" (*P-n. lineola* cf. *lineola*, *F. rhombica*, *F. pseudonana*, *N. directa* and *T. gracilis* group) and *F. kerguelensis* in the 800 and 1500 m traps of the 54°S site.

sinking algal aggregates, allowing these species to escape grazing pressure from zooplankton such as copepods and krill with longer generation times (i.e. export food web) (Quéguiner, 2013). This latter concept would also help to explain the high POC registered during summer 1999–2000, since export food webs tend to lose more organic matter via downward flux (high export efficiency) than retention food webs (low export efficiency) (Dugdale and Goering, 1967; Eppley and Peterson, 1979).

In considering these features of our results we hypothesize that the higher valve fragmentation observed in the samples during summer 1999–2000 could be due to other factors different from an intense "grazing event" as suggested previously (Closset et al., 2015). Alternatively, we venture that our sample processing technique may have selectively fragmented the valves of the weakly silicified species of the "high export group". The centrifugation of samples during sample processing for diatom slide preparation has been associated with an increase of fragments of weakly silicified and long pennate forms (Abrantes et al., 2005; Rembauville et al., 2014). Therefore, we venture that the use of the centrifuge during the sample processing in our study may have selectively fragmented the valves of the weakly silicified species of the "high export group".

In the SAZ, the duration of biomass accumulation is longer than in the PFZ, extending from October to March (up to 0.34 mg $m^{-3}$ in February) (Fig. 2b). The short pulse of BSi and diatom fluxes observed in early October in the upper trap indicates that diatoms responded rapidly to the increase of insolation and shoaling of the mixed layer in spring (Rintoul and Trull, 2001). Diatoms in the SAZ region are thought to bloom early in spring, and then be replaced by other functional groups such as *Phaeocystis*, coccolithophores and dinoflagellates (Rigual-Hernández et al., 2015b) after silicate and iron are depleted from the surface waters (Lannuzel et al., 2011). Since diatoms are only secondary contributors to the algal biomass accumulation in the SAZ waters (Kopczynska et al., 2001; de Salas et al., 2011), the determination of the time lag between algal biomass accumulation in the surface layer, BSi and diatom valve fluxes was not possible at the 47°S site.

### 4.3. Penetration of the seasonal pattern into deeper water and transport mechanisms

The seasonal pattern of the annual maxima in the BSi, POC and diatom valve fluxes registered in the shallower traps were identified in the deeper traps at both sites although in a modified form (Fig. 2). Overall, a smoothing of the seasonal signal and a time lag of the particle flux of 1–4 sampling intervals (14–50 days) were observed in the deeper traps. These shifts are most likely due to a combination of several factors, including flux attenuation between trap depths, mid-water biological activity and the descent trajectories of the particles (Buesseler et al., 2007 and references therein). The area of the surface ocean from which the particles have been produced increases with depth, i.e. the so-called "statistical funnel" defined by Siegel and Deuser (1997). Therefore, the export signal of an area of high primary production (e.g. a phytoplankton bloom) would be counterbalanced by neighbouring regions of lower production with increasing depth, smoothing out the seasonal flux pattern in the deeper traps.

The estimated settling speeds for the sinking particles between the shallow and deeper traps in the 47°S and 54°S stations during the growth season ranged between 20 and 50 m $d^{-1}$ (Fig. 2). These sinking speeds agree well with those previously estimated by Closset et al. (2015) for site 54°S and fall within the range of settling speeds of marine snow and faecal aggregates in the literature (Turner, 2002). Thus our data suggests that the sedimentation during the periods of highest flux in both the PFZ and SAZ, south of Tasmania, occurred in the form of aggregates. These observations are consistent with polyacrylamide-gel sediment traps studies where the summer flux of particles occurred principally in the form of faecal aggregates in both the PFZ and SAZ (Ebersbach et al., 2011).

A lack of visibly connected peaks and flux episodes during the autumn and winter months across the different depths, precluded the calculation of sinking rates at either of the trap sites. However, the results of Closset et al. (2015) indicate that sinking rates outside the productive period were <3 m $d^{-1}$ at the 54°S. These low velocities suggest that phytoplankton remains principally sink in the form of single cells and/or small chains during the autumn and winter months in the PFZ. This concept is consistent with the composition of the sinking diatom assemblages that were overwhelmingly dominated by the heavily silicified *Fragilariopsis kerguelensis* (up to 96% of the diatom assemblage; Fig. 3). Small and slow sinking particles are more exposed to degradation processes (e.g. silica dissolution, bacterial remineralization) during settlement than larger and rapid-sinking aggregates (Trull et al., 2008). Therefore, the enrichment of the dissolution-resistant *F. kerguelensis* during this period is most likely related to the enhanced selective dissolution of more lightly-silicified species.

### 4.4. Sources of the trap material in the SAZ site

Since *Chaetoceros* RS are often regarded as indicators of coastal environments (Abrantes, 1988; Treppke et al., 1996; Crosta et al., 1997; Takahashi et al., 2002; Rigual-Hernández et al., 2013), their presence at the 47°S site suggests that they could have been advected from a coastal region. This concept is further supported by the good correlation between the fluxes of the coastal species group (*Cocconeis* spp., *Diploneis bombus* and *Paralia* spp.) and those of *Chaetoceros* RS at all

depths ($r = 0.7$, 0.5 and 0.8 at 1000, 2000 and 3800 m, respectively). Occasional influence of coastal and subtropical waters over the study area is possible, as eddies from the East Australia Current and intermediate waters from the Tasman Outflow (a remnant of the East Australian Current) have been reported to extend as far south as the SAZ (Ridgway and Dunn, 2007; Herraiz-Borreguero and Rintoul, 2010, 2011). Thus, we interpret the occurrence of *Chaetoceros* RS and coastal taxa at the 47°S site representing the advection of hemipelagic and/or neritic water masses from the Tasmanian shelf. Nonetheless, it appears that this influence is relatively minor on the major component fluxes, based on the very low fluxes of lithogenic materials observed during the 1997–1998 deployments (Trull et al., 2001a, 2001c).

### 4.5. Comparison of the diatom assemblages in the water column and surface sediments: implications for palaeorecontructions

King and Howard (2003) analyzed the foraminiferal assemblages from the same surface sediments used in this study and concluded that the core top samples reflected the modern foraminiferal assemblages living in the overlying water masses. Despite the fact that our findings lead us to a similar conclusion, it should be noted that it is possible the top section of the piston and gravity cores may have experienced some degree of stretching or loss of material during the operation of the coring system. Thus, the surface sediment samples presented here may represent a mix of Holocene diatom assemblages rather than modern diatom assemblages.

Regardless of the sampling site, the composition of the diatom assemblages in the surface sediments unsurprisingly appears to be the result of differential dissolution of the weakly silicified taxa and consequent enrichment of robust species. Heavily-silicified diatoms such as *Fragilariopsis kerguelensis* and *Thalassiosira lentiginosa* are more likely to escape dissolution during settling and in the surface sediments, where they become overrepresented in comparison with the diatom assemblages observed in the surface layer (Kopczynska et al., 2001; de Salas et al., 2011) and captured by sediment traps (Fig. 4).

Kopczynska et al. (2001) reported that the summer diatom communities in the surface waters of the PFZ and SAZ south of Tasmania were mainly composed by the weakly silicified *Pseudo-nitzschia lineola* and *Fragilariopsis pseudonana*. At the PFZ, these species were important contributors to the sediment trap assemblages but they were completely absent in our studied surface sediments (Fig. 4a). We interpret this loss to strong dissolution in the sediment/water interface that removed their signal from the sedimentary record. Interestingly, *Pseudo-nitzschia lineola* and *Fragilariopsis pseudonana* exhibited negligible fluxes in the traps at 47°S and were not identified in the surface sediments (Fig. 4b). Therefore, our results indicate that the remineralization of weakly silicified diatoms occurs at shallower depths in the SAZ than in the PFZ. This idea is consistent with the findings of Fripiat et al. (2011) who reported that the SAZ waters south of Tasmania are more susceptible to BSi dissolution than those of the PFZ due to higher SSTs, stronger microzooplankton grazing and a more efficient microbial food web. Conversely, the higher silicate concentrations in the PFZ, less efficient dissolution (Fripiat et al., 2011) and higher silicification of the diatoms in the PFZ waters may enable a larger number of the relatively weakly silicified taxa to sink out of the mixed layer and reach the meso- and bathypelagic depths of the PFZ.

In terms of latitudinal distribution, the pattern that emerges from our core top analysis is consistent with previous reports on the biogeographic distribution of diatom species in the surface sediments of the Southern Ocean (e.g. Crosta et al., 2005; Romero et al., 2005). For example, the gradual decrease in the abundance of *F. kerguelensis* in the sediments from the PFZ (~75–90%), to the SAZ (~50–55%) and STZ (~35%) (Fig. 6) agrees well with the findings of Crosta et al. (2005) and Esper et al. (2010) who both associated the northward decline in the abundance of this species with the increase of the SST towards lower latitudes. However, other physical and chemical parameters may also play a role in the distribution of this species. Particularly, silicate concentration which is required by *F. kerguelensis* in greater concentrations in relation to other diatoms for its optimal growth (Jacques, 1983). Indeed, it is likely that the latitudinal gradient in silicate concentration in the surface waters of the Southern Ocean is largely due to the sinking and burial in the sediments of this silica sinker (Assmy et al., 2013).

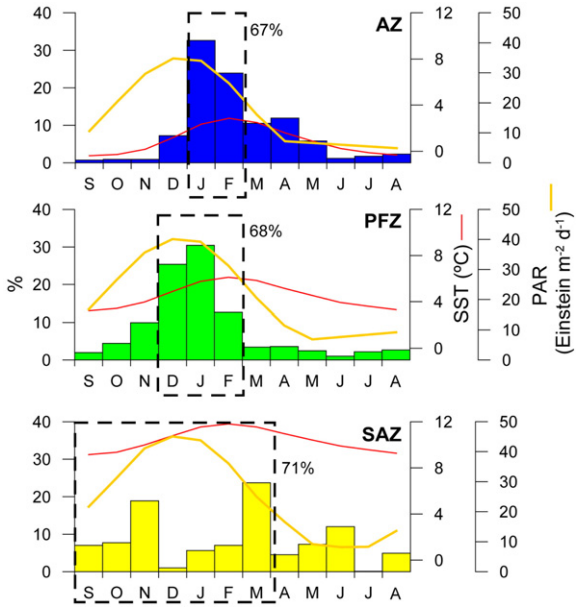


**Fig. 6.** Monthly distribution of total diatom valve flux (%) at the SAZ (47°S, 1000 m), PFZ (54°S, 800 m) and AZ (61°S, 2000 m).

The significant increase in the relative contribution of *Azpeitia tabularis*, *Hemidiscus cuneiformis* and *Roperia tesselata* in the surface sediments north of the SAF and the drop in the abundance of typical diatoms of the ACC (e.g. *T. gracilis* and *F. kerguelensis*) reflect the oligotrophic and warmer conditions of the SAZ and STZ (Romero et al., 2005). Moreover, the diatom assemblages of the surface sediments north the Subtropical Front (core top sample 6; Fig. 1a) showed significant discrepancies with those found in the sediment trap and surface sediment samples of the SAZ and PFZ (Fig. 6b). The most striking difference is the high relative contribution of *Chaetoceros* RS, which represented ~20% of the diatom assemblage at this site (Fig. 6). These results suggest that the influence of the southward flowing EAC, which carries signals of the Tasman shelf, is stronger in the STZ compared to the SAZ along 140°E. This concept is supported by the relatively high contribution of *Paralia sulcata* at this site (4%), which is often regarded as an indicator of coastal environments (McQuoid and Nordberg, 2003).

Fig. 6 shows the monthly distribution of the diatom fluxes in the shallow traps at the 47°S (1000 m), 54°S (800 m) and 61°S (2000 m) sites. The dashed intervals highlight the months required to account for two thirds of the annual diatom export, i.e. two in the AZ (January and February), three in the PFZ (December to February) and six in the SAZ (September to March). Therefore, most of the diatom valves buried in the sediments of the AZ and PFZ carry imprints of the conditions of the surface layer of the summer period, while diatom assemblages in the SAZ sediments are a reflection of the conditions of the spring and summer months, a period characterized by a greater range of variability of SSTs, PAR (Fig. 6) and nutrient concentrations (Rintoul and Trull, 2001). These observations are important for the palaeobiogeochemical studies, in particular for the calibration of new diatom-based proxies such as stable oxygen isotope ($\delta^{18}O_{Si}$) analyses on diatom valves (e.g. Shemesh et al., 2002; Swann et al., 2013). For example, oxygen isotope or trace element records obtained from diatom valves south of the SAF

should reflect SSTs conditions around their annual maximum (5–6 °C in the PFZ and 2–3 °C in the AZ). In contrast, the same stable isotope analyses undertaken at lower latitudes such as the SAZ, should mirror the surface conditions from September to March (i.e. SSTs ranging from 9–12 °C).

### 4.6. Deep carbon export in the PFZ and SAZ

The increase of the BSi:POC molar flux ratios between 800 and 1500 m at 54°S and between 1000 and 2000 m at 47°S (Table 4) reflects the faster recycling of organic carbon relative to BSi in the upper half of the water column (Nelson et al., 1996; Nelson et al., 2002). The BSi:POC ratios increased by a factor of 1.4 ± 0.0 (annual flux ± standard deviation) between 800 and 1500 m at 54°S and by a factor of 2.0 between 1000 and 2000 m at 47°S. These increasing factors of BSi:POC with depth fall within the range of those estimated by Ragueneau et al. (2002) between meso- and bathy-pelagic depths for a range of locations in the Southern Ocean (1.7 ± 0.5; average ± standard deviation) and global ocean (1.7 ± 0.4). Our results therefore confirm the findings of Ragueneau et al. (2002) who concluded that remineralization rates of BSi and POC in the Southern Ocean do not differ from other biogeochemical provinces of the world's ocean.

Rigual-Hernández et al. (2015b) identified an intimate association between the magnitude of the POC export fluxes and the composition of the sinking diatom assemblages in the shallower traps in the PFZ (Fig. 7). Highest fluxes of POC at 800 m (54°S) in the PFZ occur during the summer months in association with an elevated contribution of the "high export group". Periods of low POC export coincided with the autumn and winter months when *Fragilariopsis kerguelensis* exhibits its highest annual relative abundance. Fig. 7 shows that these relationships held true down to 1500 m. The strong positive correlation between the POC flux at 1500 m and the relative abundance of the "high export group" indicates that the largest pulses of organic matter to the deepest layers of the water column in the PFZ occur in association with "high export group" diatoms. These results agree well with the findings of Smetacek et al. (2012) during the European Iron Fertilization Experiment (EIFEX) in the iron-limited waters of the ACC. The former authors reported high numbers of *Pseudo-nitzschia lineola* (one of the main components of the "high export group") and other bloom-forming species in the underlying sediments of the patch one month after the iron addition in the form of freshly settled material. Smetacek et al. (2012) concluded that *P-n. lineola* and other boom-and-bust strategists were most likely the main contributors responsible for the deepest flux of POC during their iron fertilization experiment.

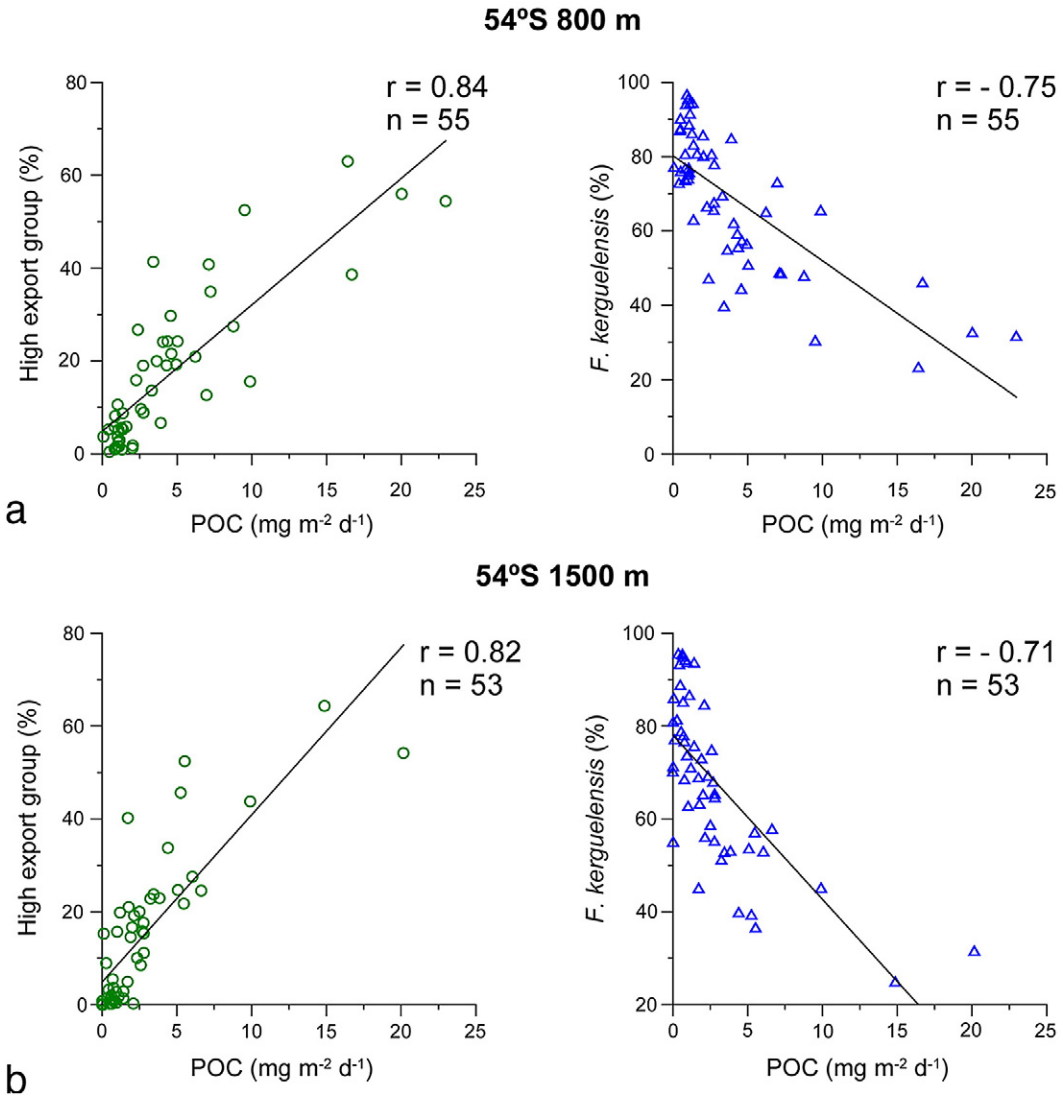


**Fig. 7.** Regression plots between the relative contribution (%) of the High Export group (*P-n. lineola* cf. *lineola*, *T. gracilis*, *F. rhombica*, *F. pseudonana* and *N. directa*) and the POC fluxes (mg $m^{-2}$ $d^{-1}$) at the 54°S site at 800 m (a) and 1500 m (b).

Our results suggest that a similar mechanism may occur for iron limited, but nonetheless diatom dominated, waters in the PFZ south of Tasmania.

The amount of POC exported to the deepest layers of the SAZ south of Tasmania is similar to that measured in the PFZ, as previously observed by Trull et al. (2001a, 2001b, 2001c) for the first year of the trap's deployment. This is despite the fact that the two zonal systems host dramatically different phytoplankton communities. The poor silica particle content registered by the sediment traps at the 47°S site (Table 4) suggest a secondary role for diatoms in the control of carbon export in this region (Closset et al., 2015; Rigual-Hernández et al., 2015b). Thus, our data indicate that a system dominated by non-siliceous phytoplankton can export the same amount of POC as a diatom-dominated ecosystem such as the PFZ. However, since photosynthesis and the biological precipitation of carbonate have opposing effects on seawater $\rho CO_2$ (Archer and Maier-Reimer, 1994; Frankignoulle et al., 1994), the higher carbonate export in the SAZ waters (Table 4; Rigual-Hernández et al., 2015b) suggests a smaller influence on surface water $\rho CO_2$ and, therefore, atmospheric $CO_2$ levels in the SAZ compared to the PFZ (Salter et al., 2014).

## 5. Conclusions

The seasonal flux pattern registered at different depths in the water column in both the SAZ and PFZ mirrored seasonal water column changes, increasing in spring along with light levels and mixed layer shallowing, and ahead of seasonal warming. Overall, a delay of about one month between maximum biomass accumulation in the surface layer and peak particulate fluxes in the shallower traps was observed at both sites. Estimated sinking rates between trap depths agree well with previous research that suggests that the particles in the meso- and bathypelagic zones at both zonal systems occur in the form of algal and/or faecal aggregates during the productive season. Higher POC export fluxes to the deepest layers of the water column at the PFZ occurred in association with a group of bloom-forming diatoms defined here as the “high export group”. Most of the members of this group of species have been previously reported to undergo cycles of rapid biomass build-up followed by mass mortality and rapid sinking during iron-fertilization experiments in the Southern Ocean. Our results therefore confirm that these boom-and-bust strategists are important contributors to naturally occurring blooms in the pelagic waters of the PFZ and are most likely the main vectors of carbon export to the deepest layers of the water column in the aftermath of the bloom. Strong dissolution in the sediment/water interface in the underlying sediments removed the signal of most of the members of the “High Export Group” leaving the sediment assemblage enriched in more heavily silicified species such as *Fragilariopsis kerguelensis*, *Thalassiosira lentiginosa* and *Chaetoceros* resting spores. Our data shows that the majority of the diatom valves buried in the sediments of the AZ and PFZ carry imprints of the conditions of the surface waters of the summer period, while those preserved in the SAZ sediments reflect the conditions of the spring and summer, a period characterized by a greater range of variability of environmental variables. These data are especially relevant for palaeoenvironmental studies, in particular when comparing diatom sedimentary records from different regions from the Southern Ocean.

## Acknowledgments

The SAZ Project sediment trap moorings have received support the Australian Antarctic Sciences awards AAS1156 and AA2256 (T. Trull), the US National Science Foundation Office of Polar Programs (R. Francois, T. Trull, S. Honjo and S. Manganini), the Belgian Science and Policy Office (F. Dehairs), CSIRO Marine Laboratories, and the Australian Integrated Marine Observing System (of which they are currently a component of the IMOS Southern Ocean Time Series Facility; www.imos.org.au). The present work was made possible by the Australian Government's Australian Antarctic Science Grant Program (Project number 4078) and Macquarie University (A. Rigual-Hernández and L. Armand). Dr Alexandra L. King (Geosciences Australia) is credited for supplying the surface sediment samples used in this study. The chlorophyll-*a* and PAR data sets and chlorophyll-*a* visualizations used in this paper were produced with the Giovanni online data system, developed and maintained by the NASA GES DISC. Diana M. Davies is thanked for performing biogeochemical analyses on the trap material. Helpful comments on an early version of the manuscript were given by Emmanuel C. Laurenceau-Cornec. Anne-Marie Ballegeer is acknowledged for her technical support in the preparation of samples and constructive comments on an early draft of the manuscript. The authors are thankful to Jessica Wilks and Kelly Lawler for their help in the microscopy analysis and taxonomic identifications. The authors acknowledge the assistance and support of Nicole Vella and Debra Birch from the Macquarie University Microscopy Unit in the scanning electron microscopy analysis. We also greatly appreciate comments and encouragement provided by Prof. Thierry Corrège and an anonymous reviewer.

## References

Abelmann, A., Gersonde, R., 1991. Biosiliceous particle flux in the Southern Ocean. Mar. Chem. 35, 503–536.
Abrantes, F., 1988. Diatom assemblages as upwelling indicators in surface sediments off Portugal. Mar. Geol. 85, 15–39.
Abrantes, F., Gil, I., Lopes, C., Castro, M., 2005. Quantitative diatom analyses—a faster cleaning procedure. Deep-Sea Res. I Oceanogr. Res. Pap. 52, 189–198.
Anderson, R.F., Ali, S., Bradtmiller, L.I., Nielsen, S.H.H., Fleisher, M.Q., Anderson, B.E., Burckle, L.H., 2009. Wind-driven upwelling in the Southern Ocean and the deglacial rise in atmospheric CO2. Science 323, 1443–1448.
Archer, D., Maier-Reimer, E., 1994. Effect of deep-sea sedimentary calcite preservation on atmospheric CO2 concentration. Nature 367, 260–263.
Armand, L.K., Leventer, A., 2010. Palaeo sea ice distribution and reconstruction derived from the geological records. Sea Ice 469-530, 2010.
Armstrong, R.A., Lee, C., Hedges, J.I., Honjo, S., Wakeham, S.G., 2002. A new, mechanistic model for organic carbon fluxes in the ocean based on the quantitative association of POC with ballast minerals. Deep-Sea Res. II Top. Stud. Oceanogr. 49, 219–236.
Assmy, P., Henjes, J., Klaas, C., Smetacek, V., 2007. Mechanisms determining species dominance in a phytoplankton bloom induced by the iron fertilization experiment EisenEx in the Southern Ocean. Deep-Sea Res. I Oceanogr. Res. Pap. 54, 340–362.
Assmy, P., Smetacek, V., Montresor, M., Klaas, C., Henjes, J., Strass, V.H., Arrieta, J.M., Bathmann, U., Berg, G.M., Breitbarth, E., Cisewski, B., Friedrichs, L., Fuchs, N., Herndl, G.J., Jansen, S., Krägefsky, S., Latasa, M., Peeken, I., Röttgers, R., Scharek, R., Schüller, S.E., Steigenberger, S., Webb, A., Wolf-Gladrow, D., 2013. Thick-shelled, grazer-protected diatoms decouple ocean carbon and silicon cycles in the iron-limited Antarctic Circumpolar Current. Proceedings of the National Academy of Sciences. 110, pp. 20633–20638.
Bacon, M.P., 1996. Evaluation of sediment traps with naturally occurring radionuclides. SCOPE 57, 85–90.
Baker, E.T., Milburn, H.B., Tennant, D.A., 1988. Field assessment of sediment trap efficiency under varying flow conditions. J. Mar. Res. 46, 573–592.
Bárcena, M.A., Abrantes, F., 1998. Evidence of a high-productivity area off the coast of Málaga from studies of diatoms in surface sediments. Mar. Micropaleontol. 35, 91–103.
Boltovskoy, D., Alder, V.A., Abelmann, A., 1993. Annual flux of radiolaria and other shelled plankters in the eastern equatorial atlantic at 853 m: seasonal variations and polycystine species-specific responses. Deep-Sea Res. I Oceanogr. Res. Pap. 40, 1863–1895.
Bowie, A.R., Lannuzel, D., Remenyi, T.A., Wagener, T., Lam, P.J., Boyd, P.W., Guieu, C., Townsend, A.T., Trull, T.W., 2009. Biogeochemical iron budgets of the Southern Ocean south of Australia: decoupling of iron and nutrient cycles in the subantarctic zone by the summertime supply. Glob. Biogeochem. Cycles 23, GB4034.
Bowie, A.R., Brian Griffiths, F., Dehairs, F., Trull, T., 2011. Oceanography of the subantarctic and Polar Frontal Zones south of Australia during summer: setting for the SAZ-Sense study. Deep-Sea Res. II Top. Stud. Oceanogr. 58, 2059–2070.
Boyd, P.W., Trull, T.W., 2007. Understanding the export of biogenic particles in oceanic waters: is there consensus? Prog. Oceanogr. 72, 276–312.
Bray, S., Trull, T.W., Manganini, S., 2000. SAZ Project Moored Sediment Traps: Results of the 1997–1998 Deployments. Antarctic Cooperative Research Centre, Hobart, Tasmania, Australia 128 pp.
Brzezinski, M.A., Phillips, D.R., Chavez, F.P., Friederich, G.E., Dugdale, R.C., 1997. Silica production in the Monterey, California, upwelling system. Limnol. Oceanogr. 42, 1694–1705.
Buesseler, K.O., 1998. The decoupling of production and particulate export in the surface ocean. Glob. Biogeochem. Cycles 12, 297–310.
Buesseler, K.O., Ball, L., Andrews, J., Cochran, J.K., Hirschberg, D.J., Bacon, M.P., Fleer, A., Brzezinski, M., 2001. Upper ocean export of particulate organic carbon and biogenic silica in the Southern Ocean along 170°W. Deep-Sea Res. II Top. Stud. Oceanogr. 48, 4275–4297.

Buesseler, K.O., Antia, A.N., Chen, M., Fowler, S.W., Gardner, W.D., Gustafsson, O., Harada, K., Michaels, A.F., der Loeff, M.R.v., Sarin, M., 2007. An assessment of the use of sediment traps for estimating upper ocean particle fuxes. J. Mar. Res. 65, 345–416.
Cassar, N., Bender, M.L., Barnett, B.A., Fan, S., Moxim, W.J., Levy, H., Tilbrook, B., 2007. The Southern Ocean biological response to aeolian iron deposition. Science 317, 1067–1070.
Chaigneau, A., Morrow, R., 2002. Surface temperature and salinity variations between Tasmania and Antarctica, 1993–1999. J. Geophys. Res. Oceans 107 (1978–2012). SRF 22-21-SRF 22-28.
Closset, I., Cardinal, D., Bray, S.G., Thil, F., Djouraev, I., Rigual-Hernández, A.S., Trull, T.W., 2015. Seasonal variations, origin and fate of settling diatoms in the Southern Ocean tracked by silicon isotope records in deep sediment traps. Glob. Biogeochem. Cycles http://dx.doi.org/10.1002/2015GB005180 (n/a-n/a, 2015).
Crosta, X., Pichon, J.-J., Labracherie, M., 1997. Distribution of Chaetoceros resting spores in modern peri-Antarctic sediments. Mar. Micropaleontol. 29, 283–299.
Crosta, X., Romero, O., Armand, L.K., Pichon, J.-J., 2005. The biogeography of major diatom taxa in Southern Ocean sediments: 2. Open ocean related species. Palaeogeogr. Palaeoclimatol. Palaeoecol. 223, 66–92.
Crosta, X., Denis, D., Ther, O., 2008. Sea ice seasonality during the Holocene, Adélie Land, East Antarctica. Mar. Micropaleontol. 66, 222–232.
de Salas, M.F., Eriksen, R., Davidson, A.T., Wright, S.W., 2011. Protistan communities in the Australian sector of the Sub-Antarctic Zone during SAZ-Sense. Deep-Sea Res. II Top. Stud. Oceanogr. 58, 2135–2149.
Deacon, G.E.R., 1982. Physical and biological zonation in the Southern Ocean. Deep Sea Res. Part A 29, 1–15.
Dugdale, R.C., Goering, J.J., 1967. Uptake of new and regenerated forms of nitrogen in primary productivity. Limnol. Oceanogr. 12, 196–206.
Dugdale, R.C., Wilkerson, F.P., 1998. Silicate regulation of new production in the equatorial Pacific upwelling. Nature 391, 270–273.
Dugdale, R.C., Wilkerson, F.P., Minas, H.J., 1995. The role of a silicate pump in driving new production. Deep-Sea Res. I Oceanogr. Res. Pap. 42, 697–719.
Ebersbach, F., Trull, T.W., Davies, D.M., Bray, S.G., 2011. Controls on mesopelagic particle fluxes in the Sub-Antarctic and Polar Frontal Zones in the Southern Ocean south of Australia in summer—perspectives from free-drifting sediment traps. Deep-Sea Res. II Top. Stud. Oceanogr. 58, 2260–2276.
Eppley, R.W., Peterson, B.J., 1979. Particulate organic matter flux and planktonic new production in the deep ocean. Nature 282, 677.
Esper, O., Gersonde, R., Kadagies, N., 2010. Diatom distribution in southeastern Pacific surface sediments and their relationship to modern environmental variables. Palaeogeogr. Palaeoclimatol. Palaeoecol. 287, 1–27.
Ferry, A.J., Prvan, T., Jersky, B., Crosta, X., Armand, L.K., 2015. Statistical modeling of Southern Ocean marine diatom proxy and winter sea ice data: model comparison and developments. Prog. Oceanogr. 131, 100–112.
Fischer, G., Gersonde, R., Wefer, G., 2002. Organic carbon, biogenic silica and diatom fluxes in the marginal winter sea-ice zone and in the Polar Front Region: interannual variations and differences in composition. Deep-Sea Res. II Top. Stud. Oceanogr. 49, 1721–1745.
Frankignoulle, M., Canon, C., Gattuso, J.-P., 1994. Marine calcification as a source of carbon dioxide: positive feedback of increasing atmospheric CO2. Limnol. Oceanogr. 39, 458–462.
Fripiat, F., Leblanc, K., Elskens, M., Cavagna, A.J., Armand, L., André, L., F., D., D., C., 2011. Efficient silicon recycling in summer in both the Polar Frontal and Subantarctic Zones of the Southern Ocean. Mar. Ecol. Prog. Ser. 435, 47–61.
Fryxell, G.A., 1994. Planktonic marine diatom winter stages: Antarctic alternatives to resting spores. Memoirs of the California Academy of Sciences. 17, pp. 437–448.
Garcia, H.E., Locarnini, R.A., Boyer, T.P., Antonov, J.I., Baranova, O.K., Zweng, M.M., Reagan, J.R., Johnson, D.R., 2014. World Ocean Atlas 2013, Volume 4: Dissolved Inorganic Nutrients (phosphate, nitrate, silicate). In: Levitus, S. (Ed.)A. Mishonov Technical Ed.; NOAA Atlas NESDIS 76, p. 25.
Gardner, W.D., 1989. Sediment trap technology and sampling. Report of the U.S. GOFS Working Group on Sediment Trap Technology and Sampling 94 pp.
Gauld, D.T., 1957. A peritrophic membrane in calanoid copepods. Nature 179, 325–326.
Gersonde, R., Zielinski, U., 2000. The reconstruction of late Quaternary Antarctic sea-ice distribution—the use of diatoms as a proxy for sea-ice. Palaeogeogr. Palaeoclimatol. Palaeoecol. 162, 263–286.
Gersonde, R., Crosta, X., Abelmann, A., Armand, L., 2005. Sea-surface temperature and sea ice distribution of the Southern Ocean at the EPILOG Last Glacial Maximum—a circum-Antarctic view based on siliceous microfossil records. Quat. Sci. Rev. 24, 869–896.
Green, S.E., Sambrotto, R.N., 2006. Plankton community structure and export of C, N, P and Si in the Antarctic Circumpolar Current. Deep-Sea Res. II Top. Stud. Oceanogr. 53, 620–643.
Grigorov, I., Rigual-Hernandez, A.S., Honjo, S., Kemp, A.E.S., Armand, L.K., 2014. Settling fluxes of diatoms to the interior of the Antarctic circumpolar current along 170°W. Deep-Sea Res. I Oceanogr. Res. Pap. 93, 1–13.
Hamm, C.E., Merkel, R., Springer, O., Jurkojc, P., Maier, C., Prechtel, K., Smetacek, V., 2003. Architecture and material properties of diatom shells provide effective mechanical protection. Nature 421, 841–843.
Herraiz-Borreguero, L., Rintoul, S.R., 2010. Subantarctic Mode Water variability influenced by mesoscale eddies south of Tasmania. J. Geophys. Res. Oceans 115, C04004.
Herraiz-Borreguero, L., Rintoul, S.R., 2011. Regional circulation and its impact on upper ocean variability south of Tasmania. Deep-Sea Res. II Top. Stud. Oceanogr. 58, 2071–2081.
Honjo, S., Francois, R., Manganini, S., Dymond, J., Collier, R., 2000. Particle fluxes to the interior of the Southern Ocean in the Western Pacific sector along 170°W. Deep-Sea Res. II Top. Stud. Oceanogr. 47, 3521–3548.
Hurd, D.C., 1972. Factors affecting solution rate of biogenic opal in seawater. Earth Planet. Sci. Lett. 15, 411–417.
Hurd, D.C., Birdwhistell, S., 1983. On producing a more general model for biogenic silica dissolution. Am. J. Sci. 283, 1–28.
Jacques, G., 1983. Some ecophysiological aspects of the Antarctic phytoplankton. Polar Biol. 2, 27–33.
Jickells, T.D., An, Z.S., Andersen, K.K., Baker, A.R., Bergametti, G., Brooks, N., Cao, J.J., Boyd, P.W., Duce, R.A., Hunter, K.A., Kawahata, H., Kubilay, N., la Roche, J., Liss, P.S., Mahowald, N., Prospero, J.M., Ridgwell, A.J., Tegen, I., Torres, R., 2005. Global iron connections between desert dust, ocean biogeochemistry, and climate. Science 308, 67–71.
Jordan, R., Stickley, C., 2010. Diatoms as Indicators of Paleoceanographic Events, the Diatoms: Applications for the Environmental and Earth Sciences. Cambridge University Press, Cambridge, p. 2010.
Kamatani, A., 1982. Dissolution rates of silica from diatoms decomposing at various temperatures. Mar. Biol. 68, 91–96.
King, A.L., Howard, W.R., 2003. Planktonic foraminiferal flux seasonality in Subantarctic sediment traps: a test for paleoclimate reconstructions. Paleoceanography 18, 1019.
Kopczynska, E.E., Dehairs, F., Elskens, M., Wright, S., 2001. Phytoplankton and microzooplankton variability between the Subtropical and Polar Fronts south of Australia: thriving under regenerative and new production in late summer. J. Geophys. Res. Oceans 106, 31597–31609.
Lannuzel, D., Bowie, A.R., Remenyi, T., Lam, P., Townsend, A., Ibisanmi, E., Butler, E., Wagener, T., Schoemann, V., 2011. Distributions of dissolved and particulate iron in the sub-Antarctic and Polar Frontal Southern Ocean (Australian sector). Deep-Sea Res. II Top. Stud. Oceanogr. 58, 2094–2112.
Lutz, M.J., Caldeira, K., Dunbar, R.B., Behrenfeld, M.J., 2007. Seasonal rhythms of net primary production and particulate organic carbon flux to depth describe the efficiency of biological pump in the global ocean. J. Geophys. Res. Oceans 112 n/a-n/a.
Martin, J.H., Knauer, G.A., Karl, D.M., Broenkow, W.W., 1987. VERTEX: carbon cycling in the Northeast Pacific. Deep-Sea Research 34, 267–285.
McCartney, M.S., 1977. Subantarctic mode water. In: Angel, M.V. (Ed.), A Voyage of Discovery. Pergamon, New York.
McQuoid, M.R., Nordberg, K., 2003. The diatom Paralia sulcata as an environmental indicator species in coastal sediments. Estuar. Coast. Shelf Sci. 56, 339–354.
Nees, S., Armand, L., De Deckker, P., Labracherie, M., Passlow, V., 1999. A diatom and benthic foraminiferal record from the South Tasman Rise (southeastern Indian Ocean): implications for palaeoceanographic changes for the last 200,000 years. Mar. Micropaleontol. 38, 69–89.
Nelson, D.M., Tréguer, P., Brzezinski, M.A., Leynaert, A., Quéguiner, B., 1995. Production and dissolution of biogenic silica in the ocean: revised global estimates, comparison with regional data and relationship to biogenic sedimentation. Glob. Biogeochem. Cycles 9, 359–372.
Nelson, D.M., DeMaster, D.J., Dunbar, R.B., Smith, W.O., 1996. Cycling of organic carbon and biogenic silica in the Southern Ocean: estimates of water-column and sedimentary fluxes on the Ross Sea continental shelf. J. Geophys. Res. Oceans 101, 18519–18532 (1978–2012).
Nelson, D.M., Anderson, R.F., Barber, R.T., Brzezinski, M.A., Buesseler, K.O., Chase, Z., Collier, R.W., Dickson, M.-L., François, R., Hiscock, M.R., Honjo, S., Marra, J., Martin, W.R., Sambrotto, R.N., Sayles, F.L., Sigmon, D.E., 2002. Vertical budgets for organic carbon and biogenic silica in the Pacific sector of the Southern Ocean, 1996–1998. Deep-Sea Res. II Top. Stud. Oceanogr. 49, 1645–1674.
Nowlin, W.D.J., Clifford, M., 1982. The kinematic and thermohaline zonation of the Antarctic Circumpolar Current at Drake Passage. J. Mar. Res. 40, 481–507.
Orsi, A.H., Whitworth Iii, T., Nowlin Jr., W.D., 1995. On the meridional extent and fronts of the Antarctic Circumpolar Current. Deep-Sea Res. I Oceanogr. Res. Pap. 42, 641–673.
Passow, U., Engel, A., Ploug, H., 2003. The role of aggregation for the dissolution of diatom frustules. FEMS Microbiol. Ecol. 46, 247–255.
Perch-Nielsen, K., 1985. Silicoflagellates. In: Bolli, H.M., Saunders, J.B., Perch-Nielsen, K. (Eds.), Plankton Stratigraphy. Cambridge Earth Science Series.
Popp, B.N., Trull, T., Kenig, F., Wakeham, S.G., Rust, T.M., Tilbrook, B., Griffiths, B., Wright, S.W., Marchant, H.J., Bidigare, R.R., Laws, E.A., 1999. Controls on the carbon isotopic composition of southern ocean phytoplankton. Glob. Biogeochem. Cycles 13, 827–843.
Quéguiner, B., 2013. Iron fertilization and the structure of planktonic communities in high nutrient regions of the Southern Ocean. Deep-Sea Res. II Top. Stud. Oceanogr. 90, 43–54.
Ragueneau, O., Tréguer, P., Leynaert, A., Anderson, R.F., Brzezinski, M.A., Demaster, D.J., Dugdale, R.C., Dymond, J., Fisher, G., François, R., Heinze, C., Maier-Reimer, E., Martin-Jézéquel, V., Nelson, D.M., Quéguiner, B., 2000. A review of the Si cycle in the modern ocean: recent progress and missing gaps in the application of biogenic opal as a paleoproductivity proxy. Glob. Planet. Chang. 26, 317–365.
Ragueneau, O., Dittert, N., Pondaven, P., Tréguer, P., Corrin, L., 2002. Si/C decoupling in the world ocean: is the Southern Ocean different? Deep-Sea Res. II Top. Stud. Oceanogr. 49, 3127–3154.
Ragueneau, O., Schultes, S., Bidle, K., Claquin, P., Moriceau, B., 2006. Si and C interactions in the world ocean: importance of ecological processes and implications for the role of diatoms in the biological pump. Glob. Biogeochem. Cycles 20, GB4S02.
Rembauville, M., Blain, S., Armand, L., Quéguiner, B., Salter, I., 2014. Export fluxes in a naturally fertilized area of the Southern Ocean, the Kerguelen Plateau: ecological vectors of carbon and biogenic silica to depth (part 2). Biogeosci. Discuss. 11, 17089–17150.
Ridgway, K.R., Dunn, J.R., 2007. Observational evidence for a southern hemisphere oceanic supergyre. Geophys. Res. Lett. 34, L13612.

Rigual-Hernández, A.S., Bárcena, M.A., Jordan, R.W., Sierro, F.J., Flores, J.A., Meier, K.J.S., Beaufort, L., Heussner, S., 2013. Diatom fluxes in the NW Mediterranean: evidence from a 12-year sediment trap record and surficial sediments. J. Plankton Res. 35, 1109–1125.

Rigual-Hernández, A.S., Trull, T.W., Bray, S.G., Closset, I., Armand, L.K., 2015a. Seasonal dynamics in diatom and particulate export fluxes to the deep sea in the Australian sector of the southern Antarctic Zone. J. Mar. Syst. 142, 62–74.

Rigual-Hernández, A.S., Trull, T.W., Bray, S.G., Cortina, A., Armand, L.K., 2015b. Latitudinal and temporal distributions of diatom populations in the pelagic waters of the Subantarctic and Polar Frontal Zones of the Southern Ocean and their role in the biological pump. Biogeosci. Discuss. 12, 8615–8690.

Rintoul, S.R., Trull, T.W., 2001. Seasonal evolution of the mixed layer in the Subantarctic zone south of Australia. J. Geophys. Res. Oceans 106, 31447–31462.

Romero, O., Armand, L., 2010. Marine diatoms as indicators of modern changes in oceanographic conditions. In: Smol, J.P., Stoermer, E.F. (Eds.), The Diatoms: Applications for the Environmental and Earth Sciences.

Romero, O.E., Armand, L.K., Crosta, X., Pichon, J.J., 2005. The biogeography of major diatom taxa in Southern Ocean surface sediments: 3. Tropical/Subtropical species. Palaeogeogr. Palaeoclimatol. Palaeoecol. 223, 49–65.

Romero, O.E., Thunell, R.C., Astor, Y., Varela, R.A., 2009. Seasonal and interannual dynamics in diatom production in the Cariaco Basin, Venezuela. Deep-Sea Res. I Oceanogr. Res. Pap. 56, 571–581.

Rynearson, T.A., Richardson, K., Lampitt, R.S., Sieracki, M.E., Poulton, A.J., Lyngsgaard, M.M., Perry, M.J., 2013. Major contribution of diatom resting spores to vertical flux in the sub-polar North Atlantic. Deep-Sea Res. I Oceanogr. Res. Pap. 82, 60–71.

Sackett, O., Armand, L., Beardall, J., Hill, R., Doblin, M., Connelly, C., Howes, J., Stuart, B., Ralph, P., Heraud, P., 2014. Taxon-specific responses of Southern Ocean diatoms to Fe enrichment revealed by synchrotron radiation FTIR microspectroscopy. Biogeosciences 11, 5795–5808.

Salter, I., Kemp, A.E.S., Moore, C.M., Lampitt, R.S., Wolff, G.A., Holtvoeth, J., 2012. Diatom resting spore ecology drives enhanced carbon export from a naturally iron-fertilized bloom in the Southern Ocean. Glob. Biogeochem. Cycles 26, GB1014.

Salter, I., Schiebel, R., Ziveri, P., Movellan, A., Lampitt, R., Wolff, G.A., 2014. Carbonate counter pump stimulated by natural iron fertilization in the Polar Frontal Zone. Nat. Geosci. 7, 885–889.

Sancetta, C., 1989. Spatial and temporal trends of diatom flux in British Columbian fjords. J. Plankton Res. 11, 503–520.

Sancetta, C., Calvert, S.E., 1988. The annual cycle of sedimentation in Saanich inlet, British Columbia: implications for the interpretation of diatom fossil assemblages. Deep Sea Res. Part A 35, 71–90.

Sarmiento, J.L., Gruber, N., Brzezinski, M.A., Dunne, J.P., 2004. High-latitude controls of thermocline nutrients and low latitude biological productivity. Nature 427, 56–60.

Shemesh, A., Hodell, D., Crosta, X., Kanfoush, S., Charles, C., Guilderson, T., 2002. Sequence of events during the last deglaciation in Southern Ocean sediments and Antarctic ice cores. Paleoceanography 17 8-1-8-7.

Shiono, M., Koizumi, I., 2000. Taxonomy of the *Thalassiosira trifulta* group in late neogene sediments from the northwest Pacific Ocean. Diatom Research 15, 355–382.

Siegel, D.A., Deuser, W.G., 1997. Trajectories of sinking particles in the Sargasso Sea: modeling of statistical funnels above deep-ocean sediment traps. Deep-Sea Res. I Oceanogr. Res. Pap. 44, 1519–1541.

Smetacek, V., Klaas, C., Strass, V.H., Assmy, P., Montresor, M., Cisewski, B., Savoye, N., Webb, A., d/'Ovidio, F., Arrieta, J.M., Bathmann, U., Bellerby, R., Berg, G.M., Croot, P., Gonzalez, S., Henjes, J., Herndl, G.J., Hoffmann, L.J., Leach, H., Losch, M., Mills, M.M., Neill, C., Peeken, I., Rottgers, R., Sachs, O., Sauter, E., Schmidt, M.M., Schwarz, J., Terbruggen, A., Wolf-Gladrow, D., 2012. Deep carbon export from a Southern Ocean iron-fertilized diatom bloom. Nature 487, 313–319.

Sokolov, S., Rintoul, S.R., 2002. Structure of Southern Ocean fronts at 140°E. J. Mar. Syst. 37, 151–184.

Sokolov, S., Rintoul, S.R., 2009a. Circumpolar structure and distribution of the Antarctic Circumpolar Current fronts: 1. Mean circumpolar paths. J. Geophys. Res. Oceans 114, C11018.

Sokolov, S., Rintoul, S.R., 2009b. Circumpolar structure and distribution of the Antarctic Circumpolar Current fronts: 2. Variability and relationship to sea surface height. J. Geophys. Res. Oceans 114, C11019.

Swann, G.E.A., Pike, J., Snelling, A.M., Leng, M.J., Williams, M.C., 2013. Seasonally resolved diatom δ18O records from the West Antarctic Peninsula over the last deglaciation. Earth Planet. Sci. Lett. 364, 12–23.

Tagliabue, A., Sallee, J.-B., Bowie, A.R., Levy, M., Swart, S., Boyd, P.W., 2014. Surface-water iron supplies in the Southern Ocean sustained by deep winter mixing. Nat. Geosci. 7, 314–320.

Takahashi, K., Fujitani, N., Yanada, M., 2002. Long term monitoring of particle fluxes in the Bering Sea and the central subarctic Pacific Ocean, 1990–2000. Prog. Oceanogr. 55, 95–112.

Tréguer, P.J., 2014. The Southern Ocean silica cycle. Compt. Rendus Geosci. 346, 279–286.

Tréguer, P.J., De La Rocha, C.L., 2013. The world ocean silica cycle. Ann. Rev. Mar. Sci. 5, 477–501.

Tréguer, P., Nelson, D.M., Van Bennekom, A.J., Demaster, D.J., Quéguiner, B., Leynaert, A., 1995. The silica budget of the World Ocean: a re-estimate. Science 268, 375–379.

Treppke, U.F., Lange, C.B., Wefer, G., 1996. Vertical fuxes of diatoms and silicofagellates in the eastern equatorial Atlantic, and their contribution to the sedimentary record. Mar. Micropaleontol. 28, 73–96.

Trull, T.W., Bray, S.G., Manganini, S.J., Honjo, S., François, R., 2001a. Moored sediment trap measurements of carbon export in the Subantarctic and Polar Frontal zones of the Southern Ocean, south of Australia. J. Geophys. Res. Oceans 106, 31489–31509.

Trull, T.W., Rintoul, S.R., Hadfield, M., Abraham, E.R., 2001b. Circulation and seasonal evolution of polar waters south of Australia: implications for iron fertilization of the Southern Ocean. Deep-Sea Res. II Top. Stud. Oceanogr. 48, 2439–2466.

Trull, T.W., Sedwick, P.N., Griffiths, F.B., Rintoul, S.R., 2001c. Introduction to special section: SAZ Project. J. Geophys. Res. Oceans 106, 31425–31429.

Trull, T.W., Bray, S.G., Buesseler, K.O., Lamborg, C.H., Manganini, S., Moy, C., Valdes, J., 2008. In situ measurement of mesopelagic particle sinking rates and the control of carbon transfer to the ocean interior during the Vertical Flux in the Global Ocean (VERTIGO) voyages in the North Pacific. Deep-Sea Res. II Top. Stud. Oceanogr. 55, 1684–1695.

Turner, J.T., 2002. Zooplankton fecal pellets, marine snow and sinking phytoplankton blooms. Aquat. Microb. Ecol. 27, 57–102.

Wright, S.W., Thomas, D.P., Marchant, H.J., Higgins, H.W., Mackey, M.D., Mackey, D.J., 1996. Analysis of phytoplankton of the Australian sector of the Southern Ocean: comparisons of microscopy and size frequency data with interpretations of pigment HPLC data using the 'CHEMTAX' matrix factorisation program. Mar. Ecol. Prog. Ser. 144, 285–298.

Yoon, W., Kim, S., Han, K., 2001. Morphology and sinking velocities of fecal pellets of copepod, molluscan, euphausiid, and salp taxa in the northeastern tropical Atlantic. Mar. Biol. 139, 923–928.

Yu, E.F., Francois, R., Bacon, M.P., Honjo, S., Fleer, A.P., Manganini, S.J., Rutgers van der Loeff, M.M., Ittekot, V., 2001. Trapping efficiency of bottom-tethered sediment traps estimated from the intercepted fluxes of 230Th and 231 Pa. Deep-Sea Res. I Oceanogr. Res. Pap. 48, 865–889.